Environmental Security Technology Certification Program

(ESTCP)

Final Report
Version 2
Project: MM-0604

Small Area Inertial Navigation Tracking (SAINT) System for Precise Location of Buried UXO

July 2007

Approved for public release; distribution is unlimited

REPORT DOCUMENTATION PAGE

Form Approved
OMB No. 0704-0188

1. REPORT DATE *(DD-MM-YYYY)*	**2. REPORT TYPE**	**3. DATES COVERED** *(From - To)*
16-07-2007	Final Report Version 2	03/2006-07/2007

4. TITLE AND SUBTITLE
Small Area Inertial Navigation Tracking (SAINT) System for

Location of Buried UXO

5a. CONTRACT NUMBER

5b. GRANT NUMBER
W912DY-06-2-0101

5c. PROGRAM ELEMENT NUMBER

6. AUTHOR(S)
Jane Bohlin, David Taylor, Scott Millhouse

5d. PROJECT NUMBER
ESTCP 200604

5e. TASK NUMBER

5f. WORK UNIT NUMBER

7. PERFORMING ORGANIZATION NAME(S) AND ADDRESS(ES)

ENSCO Inc.
5400 Port Royal Road
Springfield, VA 22151-2312

8. PERFORMING ORGANIZATION REPORT NUMBER

9. SPONSORING / MONITORING AGENCY NAME(S) AND ADDRESS(ES)
US Army Corps of Engineers
USAESCH, Huntsville
Box 1600
Huntsville, AL 35807-4301

10. SPONSOR/MONITOR'S ACRONYM(S)
USAESCH

11. SPONSOR/MONITOR'S REPORT NUMBER(S)

12. DISTRIBUTION / AVAILABILITY STATEMENT

Distribution not limited

13. SUPPLEMENTARY NOTES

14. ABSTRACT

This report documents a demonstration at Aberdeen Proving Grounds on September 12-13, 2006 of the second generation SAINT inertial navigation positioning technology integrated with an EM61-HH metal detector. The primary objective of this demonstration was to demonstrate a relative position accuracy of the EM61-HH sensor of less than 2 cm (one standard deviation) along each of the three axes of the local positioning reference frame. The primary motivation for SAINT is to reduce the cost of OE remediation, which, in large part, is driven by the excavation costs of non-hazardous targets.

SAINT was demonstrated to produce relative positioning accuracy of less than 5 mm and inversion fit quality consistent with a <1 cm positional accuracy. This accuracy is expected to be sufficient to allow target characterization based upon the EM61-HH sensor data tied to accurate relative geolocation. During the demonstration, data were collected at a rate of 6 targets per hour for a single operator. In production use we anticipate a minimum rate of 12 targets per hour. This production rate is expected to result in an interrogation cost of $7 per target, thus potentially saving a substantial percentage of OE remediation costs.

15. SUBJECT TERMS
Inertial Positioning, Interrogation, Discrimination, UXO

16. SECURITY CLASSIFICATION OF: Unclassified			**17. LIMITATION OF ABSTRACT**	**18. NUMBER OF PAGES**	**19a. NAME OF RESPONSIBLE PERSON**
a. REPORT	**b. ABSTRACT**	**c. THIS PAGE**	UU	58	Scott Millhouse
					19b. TELEPHONE NUMBER *(include area code)* 256-895-1607

Standard Form 298 (Rev. 8-98)
Prescribed by ANSI Std. Z39.18

Table of Contents

List of Acronyms

2D	Two-dimensional
3D	Three-dimensional
APG	Aberdeen Proving Grounds
CEHNC	Corps of Engineers Huntsville Center
CF	Compact flash
cm	Centimeter
DGM	Digital geophysical mapping
EDM	Electronic distance measurement (laser)
ESTCP	Environmental Security Technology Certification Program
ft	Foot
GHz	Gigahertz
GPS	Global positioning system
IMU	Inertial measurement unit
INS	Inertial navigation system
ISM	Industrial, Scientific and Medical
kbps	Kilo-bits per second
lb	Pound
m	Meter
MD	Maryland
MEMS	Microelectromechanical system
MK-2	Mark-2
mm	Millimeter
ms	Millisecond
mV	Millivolt
OE	Ordnance and explosives
PC	Personal computer
SAINT	Small area inertial navigation tracking system
UXO	Unexploded ordnance
ZUPT	Zero velocity update

List of Figures

List of Tables

Acknowledgements

This project was jointly funded by the U.S. Army Corps of Engineers – Huntsville Center, the Environmental Security Technology Certification Program, and ENSCO, Inc. Their continuing support is gratefully acknowledged. The staff at Aberdeen Proving Grounds provided excellent support facilitating the demonstration.

Abstract

Geophysical technologies for supporting ordnance and explosive (OE) waste remediation have focused on the problems of detecting, locating, and mapping the presence of underground objects. Experience has shown that the majority of underground objects detected by these systems presents no safety hazard and do not need to be excavated. If reliable means of distinguishing hazardous from non-hazardous objects could be developed, significant OE remediation programs' resources could be saved and more effectively deployed to mitigate safety hazards.

ENSCO, Inc. conducted a demonstration at Aberdeen Proving Grounds on September 12-13, 2006 of the second generation SAINT inertial navigation positioning technology integrated with an EM61-HH metal detector. The primary objective of this demonstration was to demonstrate a relative position accuracy of the EM61-HH sensor of less than 2 cm (one standard deviation) along each of the three axes of the local positioning reference frame.

The primary motivation for SAINT is to reduce the cost of OE remediation, which, in large part, is driven by the excavation costs of non-hazardous targets. There are no relevant regulatory drivers or constraints.

SAINT was demonstrated to produce relative positioning accuracy of less than 5 mm and inversion fit quality consistent with a <1 cm positional accuracy. This accuracy is expected to be sufficient to allow target characterization based upon the EM61-HH sensor data tied to accurate relative geolocation. During the demonstration, data were collected at a rate of 6 targets per hour for a single operator. In production use we anticipate a minimum rate of 12 targets per hour. This production rate is expected to result in an interrogation cost of $7 per target, thus potentially saving a substantial percentage of OE remediation costs.

1. Introduction

1.1 Background

Geophysical technologies for supporting ordnance and explosive (OE) waste remediation have focused on the problems of detecting, locating, and mapping the presence of underground objects. Experience has shown that the majority of underground objects detected by these systems presents no safety hazard and do not need to be excavated. If reliable means of distinguishing hazardous from non-hazardous objects could be developed, significant OE remediation programs resources could be saved and more effectively deployed to mitigate safety hazards.

Other researchers have shown a likelihood of being able to characterize buried targets via sophisticated inversion algorithms. These algorithms require high-fidelity sensor systems combined with high-fidelity positioning systems. Existing sensor technologies provide good quality sensor data, but practical high-resolution positioning systems (on the order of 1 cm error) remain a challenge.

ENSCO previously implemented and demonstrated a Small Area Inertial Navigation and Tracking System (SAINT). The first generation SAINT (Phase-I) was combined with a G-858 magnetometer. The breadboard prototype was successfully demonstrated at Aberdeen Proving Grounds (APG) in 2004, providing an average accuracy of two to four centimeters. The second generation SAINT (Phase-II) is integrated with an EM61-HH metal detector and was demonstrated at Aberdeen Proving Grounds on September 12-13, 2006.

1.2 Objectives of the Demonstration

This demonstration highlighted the integration of SAINT, an inertial based navigation system, with a standard EM61-HH metal detector. The primary objective of this demonstration was to verify the 3D positioning accuracy of the EM61-HH sensor provided by SAINT. Because no communication is needed with auxiliary components or satellites, normal operation is not effected by heavy vegetation, elevation change, water, or tree-cover, as it is the case for most other positioning systems. During post-processing the EM61-HH data was merged with the SAINT position data. However, the overall performance of the EM61-HH was not assessed; the focus was on the position accuracy.

The demonstration was conducted in the calibration grid at Aberdeen Proving Grounds (APG). The demonstration included the interrogation of 23 targets in the calibration grid. Post-processing provided EM61-HH data merged with 3D position data for the 23 targets in the calibration grid with all positions referenced in the UTM coordinates. Model-based electromagnetic inversion fit statistics are provided in Appendix E as a result of an independent evaluation of the system by SAIC (formerly AETC, Inc.).

Success was defined as demonstrating relative position errors of the sensor coil of less than 2 cm at 1 standard deviation along each of the three axes of the local positioning reference frame. Secondary demonstration objectives of the demonstration were to show robustness and reliability of the system, ease of use, and simplicity of post-processing. For a full list of demonstration objectives see Table 3.

1.3 Regulatory Drivers

This project was primarily motivated by the desire for more efficient and accurate ordnance and explosives (OE) field operations, to achieve both better technical remediation performance, and to reduce cost. Precise positioning technology is an important part of the infrastructure of OE remediation efforts, an enabling tool to allow faster, better and cheaper detection, characterization, and excavation. Thus, the need for this technology is not primarily driven by regulatory issues.

1.4 Stakeholder/End-User Issues

This demonstration report documents the relative positioning accuracy and land-area survey rate of the inertial navigation technology. Logistical issues (which are critical to OE operations) were demonstrated by documenting activities required to complete the demonstration. Cost of the technology was estimated and compared to existing technology.

Thus, the outcome of this demonstration provides end-users with an understanding of the technical, logistical, and financial impact of this technology, allowing informed decision-making by end users.

2. Technology Description

2.1 Technology Development and Application

SAINT is the small area inertial navigation tracking system. It is a stand-alone unit that can be attached to virtually any system when a recorded free navigation position trace in 3D is desired. In this demonstration, SAINT was attached to a commercially available EM61-HH (MK-2) metal detector to record free-navigation position. The purpose was to record location and orientation of the metal detector sensor head as it was arbitrarily swept over a local area where a UXO was suspected to be buried. This allows a detailed map of metal detector and position data (DGM) to be generated.

The primary positioning system consists of a Honeywell HG1900 inertial measurement unit (IMU) and a LEICA digital magnetic compass (DMC) as shown in Figure 1. SAINT also includes the following support hardware:

- Rabbit embedded CPU
- Weather-proof enclosure with mounting brackets
- Battery power-pack in satchel
- CF card
- Cables for power and data

IMU

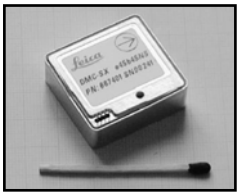

DMC

Figure 1: Honeywell HG1900 IMU and LEICA DMC

The Honeywell HG1900 IMU consists of orthogonally aligned MEMS accelerometers and gyroscopes that record 3-axis acceleration and rotation rates, respectively enclosed in an 8-cubic inch container. The LEICA DMC is employed to aid the IMU and constrain heading drift. The digital magnetic compass measures the strength and direction of a magnetic field and can be used to determine magnetic north in an environment free of additional magnetic fields. With the exception of batteries, a tripod stand, and the post-processing personal computer (PC), all components of SAINT are packaged into a single enclosure. The enclosure clamps onto the shaft of the EM61-HH, needing no special modifications, as shown in Figure 2. An additional clamp is used to fix the sensor coil relative to IMU so the position and angle offset remains constant.

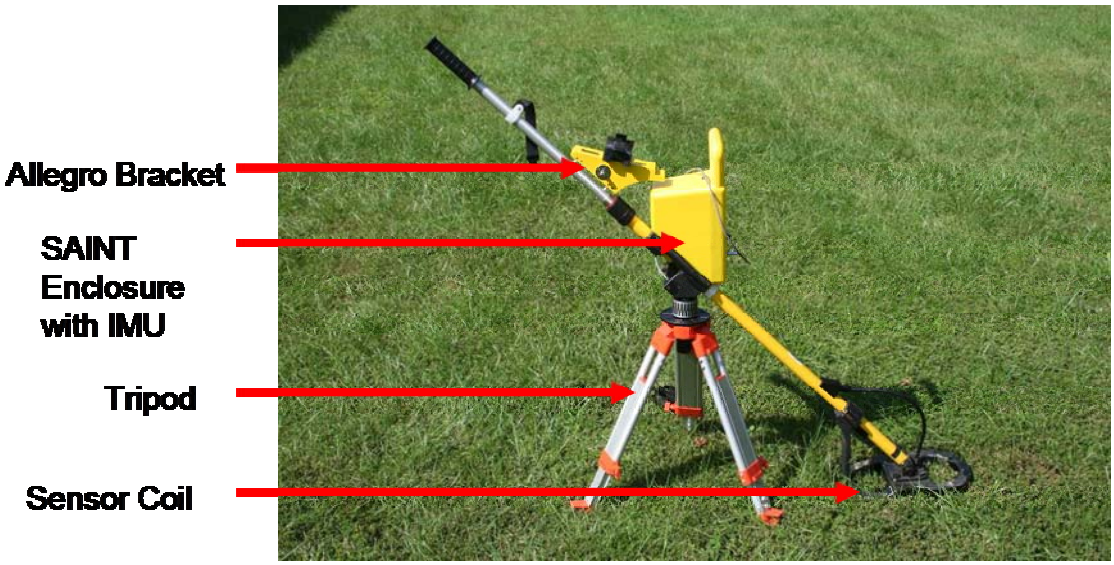

Figure 2: SAINT integrated with the EM61-HH

SAINT records all IMU data onto an internal compact flash card (CF). Digital magnetic compass data is recorded to the same CF card. This greatly simplifies user operation and data post-processing. A schematic of the integrated system is shown in Figure 3.

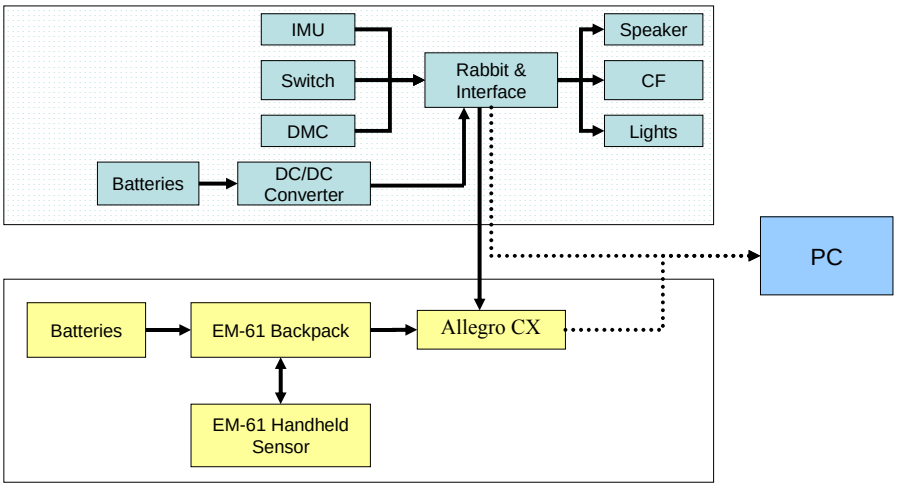

Figure 3: SAINT and EM61-HH integration schematic. Yellow components are part of the COTS EM-61 HH MK2.

The Rabbit, a single board computer based on an extension of the z-80 processor, controls the data flow, buttons, and status lights. Lights and audible signals (speaker) aid the user for proper operation.

For a solely IMU-based positioning system, best case position errors will grow as a random walk due to accumulated errors in dead reckoning speed and heading assuming all sensor biases are known and subtracted. Highly correlated errors (biases) will result in position errors that grow as

a quadratic with time. The fundamental design goals for a dead reckoning system are to minimize the heading and speed error growth by using a combination of high quality (low noise) sensors and exploiting locally available information to remove biases from these sensors. By integrating a compass and requiring that the SAINT unit remains stationary over the same point for at least 15 seconds before and after each cycle of data acquisition, a Kalman filter and Rauch-Tung-Streibel (R-T-S) Smoother (Rauch, 1965) can be used to optimally estimate and remove sensor biases and minimize position and heading errors. In addition to the heading measurement provided by the compass, the software exploits the fact that during the stationary period the IMU occupies the same position and does not move, providing a zero-velocity update (ZUPT) and position update, respectively.

Data Acquisition

Geophysical data are acquired in 30-second cycles after which the IMU must be returned to its initial position. Each cycle consists of the following steps:

1. Initial ZUPT period: The SAINT unit is set down on the tripod mount and remains stationary for 15-30 seconds.
2. Operator picks up the unit and acquires geophysical data for approximately 30 seconds of free navigation over the area of interest.
3. Final ZUPT period: The SAINT unit is returned to its original location on the tripod mount for about 15-30 seconds.

Lights and audible signals aid the user for proper operation. During the 30 second free navigation period, various audible chirps are sounded with 10, 5, and 0 seconds remaining before a new ZUPT is required. Adequate data density over a small area can be achieved by collecting multiple cycles of data.

Since there is no required infrastructure setup, data acquisition over multiple points spread over large areas can be performed quickly and efficiently by a single operator. Since the IMU rests directly above the center of the tripod, the location of the tripod defines the origin of the frame for the processed sensor position.

After all IMU data has been recorded, the SAINT CF card is removed and the data transferred to a PC using a USB CF card reader.

Data Processing

Prior to using the SAINT system for the first time, a measurement must be obtained of the three-dimensional position offset of the center of sensitivity of the EM61-HH, which is defined to be the physical center of mass of the figure-eight coil configuration, with respect to the IMU in the measurement frame of the IMU. Currently, this measurement is made in the lab. However, a calibration procedure has been developed and initially tested that estimates the relative position of the IMU to the pivot point, the center of the horizontal screw connecting the sensor head to the attached pole and then translates that position to the center of sensitivity of the EM61-HH. The center of sensitivity is located approximately 5 cm beneath the center of this screw when the coils are horizontal (note that the pole orientation relative to the coil is fixed). This calibration procedure consists of keeping the pivot stationary while pitching and yawing through 180 degrees of motion over 10 seconds and then returning the IMU to its starting location. Since the

IMU measures both three-dimensional position and attitude, it is only necessary that this pivot point does not move (rotate or translate) relative to the IMU while you pitch, yaw and translate the IMU. A statistical estimate of the position offset is computed using a Kalman filter that relies on the conditions that the IMU is rotated as described, the sensor remains stationary and the range from the sensor to the IMU remains fixed.

The data processing exploits the operational requirement that the start and stop locations of the SAINT hardware be identical. The operator can free navigate for 30 seconds, at which time the unit must be returned to the same place it started. ENSCO has implemented a ZUPT-ing tripod to simplify the return of the hardware to the identical location. Upon completion of the ZUPT, a blue indicator light illuminates on the SAINT enclosure signifying the operator can free-navigate when ready.

The post-processing software has been mostly automated and includes a GUI that requires the user to select the EM61-HH data and IMU data files for processing and the periods to process. The processing consists of the following components:

1. A pre-filter for detection of ZUPT intervals
2. Navigation equations and a Kalman filter (Rogers, 2000)
3. A R-T-S Smoother
4. A component to translate the IMU position & attitude to the geophysical sensor based on the static 3-D position & orientation offset vectors
5. A component to interpolate the sensor position & attitude (recorded at up to 600 Hz) to the recorded EM61 times (recorded at approximately 15 Hz)

The error-state Kalman filter feeds corrections back into the navigation equations for both navigation errors and IMU sensor errors to optimally estimate the position and orientation of the IMU. The accuracy of these corrections is primarily a function of the quality of the IMU, the quality of the aiding measurements to the IMU and the quality of the model defining the IMU in the Kalman filter. The accuracy of the reported errors is primarily a function of the quality of the model defining the IMU. Since the IMU contains six sensors, and each has errors from bias, drift, alignment, scale factor, nonlinearity, asymmetry, and other sources, more than 50 states in the Kalman Filter may be necessary to optimally model the IMU. For this project, the IMU was sub-optimally modeled and the Kalman filter error model (Rogers, 2000) was limited to the following 15 states:

- δr is a 3-element vector of north, east, down position errors,
- δv is a 3-element vector of north, east, down velocity errors,
- $\delta \psi$ is a 3-element vector of infinitesimal angles describing the misalignment relative to earth,
- δb^{acc} is a 3-element vector of time-correlated accelerometer errors,
- δb^{gyro} is a 3-element vector of time-correlated gyro errors,

The Kalman filter provides an optimal estimate of position based on all measurements available until time t_k. However, additional information contained in the measurements after t_k can further improve the estimate of position. A Rauch-Tung-Streibel (R-T-S) Smoother was implemented

as an algorithm to be used in post-processing that computes an optimal smoothed path estimate utilizing all available measurements within the data set (Rauch et al, 1965).

In addition to the position and attitude estimates, the error estimates are provided for each of the components of position and attitude. Processing software outputs positions in a relative coordinate system with the origin at the ZUPT location and the orientation constrained by the compass.

Concept of Operations

The concept of operations assumes the operator has a sequence of target locations, likely marked by pin flags that need to be investigated. Data are collected separately for each pin flag location; a new ZUPT location may be chosen for each pin flag location. The ZUPT location can be anywhere near the target location. The ZUPT location must remain stationary during the entire interrogation of a target. A flat, easily accessible spot is best. Assuming flags are used to mark the areas for interrogation during a survey, the procedure will consist of co-locating the ZUPT position with the flags by placing the ZUPT stand directly on top of the flagged point. Processing software outputs positions in a relative UTM coordinate system with the origin at the ZUPT location and the orientation constrained by the compass. The intent of the SAINT system is to provide accurate positions in a relative frame for interrogation algorithms; hence, there is no requirement for knowledge of the UTM position of the ZUPT point. Knowledge of the UTM position of the ZUPT point simply provides a way to map these relative positions to a UTM frame during field operations.

2.2 Previous Testing of the Technology

A demonstration of SAINT was performed at Aberdeen Proving Grounds (MD) in 2004 under ESCTP project #200129. For that demonstration, a tactical grade Honeywell HG1700 IMU was paired with a G-858 Cesium magnetometer.

Static inertial measurements were recorded at 36 marked locations within a one square meter grid, as shown by the asterisks in Figure 4. The sensor was placed in the grid locations using PVC standoffs of known length and placing the base of the standoff on marks on the plywood board defining the grid. The coordinate results recorded by SAINT were compared to actual coordinates of the fixed grid and are summarized in Table 1.

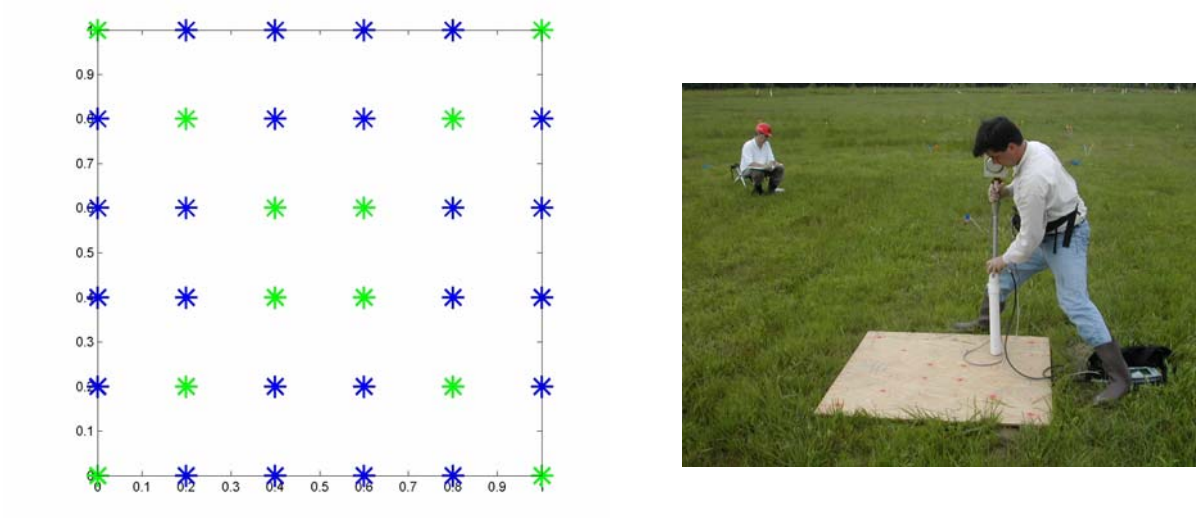

Figure 4: Static test grid design with multiple elevations recorded across the diagonals (left) and picture of actual operation including SAINT system and PVC standoff(right)

Static	Mean 2D Error (m)	Mean Altitude Error (m)
Inertial/G-858: 15 cm height	.029	.019
Inertial/G-858: 30 cm height	.040	.012
Inertial/G-858: 45 cm height	.045	.035

Table 1: Mean errors from static fixed grid testing. 2D error is defined to be the square root of the sum of the squares of the errors in the horizontal axes.

A substantial portion of these errors were likely due to the test methodology (e.g., warping of the plywood board, inaccuracy of placing the stand-off fixtures on the board, etc.) and not the geolocation method; the position accuracy of the system could not adequately be measured by the test.

Dynamic 3D SAINT testing was performed in the same grid as in the previous static test. The dynamic data set was acquired by swinging the SAINT system over an anomaly array board with an area of 1.2 m square created with an irregular array of nails inserted (point into the ground) for point source anomalies. This board was then randomly placed in an area clear of subsurface anomalies and data were acquired over the board using the integrated inertial/G-858 system. A plot was then generated of the magnetic field strength as a function of time. Magnetic anomaly peaks were selected and the corresponding times were used to linearly interpolate the reported coordinates based on the coordinates for the nearest times before and after the anomaly peak. Comparison of the selected coordinates for the points with the ground truth locations reveals the mean radial (2D) error shown in Table 2.

Dynamic	Mean 2D Error (m)
Inertial/G-858 nail board test	0.051

Table 2: This table represents the mean 2D error in the selected coordinates of the nails based on the inertial data as compared to ground truth coordinates.

Although a fixed latency was estimated, a variable latency within the EM61-HH system limited the position accuracy of the system.

2.3 Factors Affecting Cost and Performance

The major cost drivers for this system are the IMU and the quantity-one enclosure fabrication expense typical of prototype design. Larger production quantities will significantly reduce the cost per enclosure. The IMU used has not yet entered commercial production, so price per unit at moderate and large quantities is not available.

The most significant factor affecting cost and performance is the data production rate: how many sites an operator can interrogate during a fixed period of time. It is expected that this method will show significant time and cost savings as compared to laser surveying or other manual methods.

For this Phase II demonstration, application costs and productivity are recorded and compared. This includes items such as: a) daily/weekly/monthly technology costs for rental, purchase and maintenance b) technology availability and downtime considerations; c) survey productivity factors that include setup, survey area limitations, operating personnel labor requirements, cost and d) data processing considerations for position and geophysical instrument integration.

2.4 Advantages and Limitations of the Technology

The strength of SAINT is that it provides accurate positioning data over a localized area in a self-contained system. No satellites or external radios are used, so operation is not limited by any terrain or environment considerations. With accurate position data, it is expected that detailed sensor data analysis and inversion will allow buried objects to be characterized; providing this accurate position data to support target characterization is the primary objective of SAINT.

The main limitation of SAINT is the duration of free navigation time before the system must be set down and a ZUPT performed. Longer data collection times would facilitate use and decrease total operation time. IMU position errors grow quadratically with the duration of free navigation between ZUPTs. For a given IMU, shorter free navigation leads to smaller maximum errors, longer free navigation leads to larger free navigation errors. A better quality IMU would extend the useable free navigation time and/or reduce the maximum error. We selected the HG1900 as a tradeoff between price, size/weight, and performance of available IMUs.

An additional limitation to the current system that drives the positioning accuracy is the variable latency within the EM61-HH system. In standard UXO remediation the cumulative latency is

assumed to be fixed. While this may hold true at a macro level, at a millisecond level there exist variable latencies within the EM61 that affect the time correlation between the calculated positions and the measured EM61 data. One primary source of variable latency is the clock in the Allegro, the EM61 data storage device, which has a 9 millisecond resolution. Additional variability between samples is generated by the EM61 operating system and processing load of the Allegro. This creates further difficulty in locating the actual sample location.

The IMU clock (stable to 1ppm) is used for timing because it is the most precise in the SAINT system. Timing between the IMU and geophysical sensor is achieved using a NMEA GPGGA message for synchronization between the SAINT unit and the Allegro. The GPGGA message contains a time correlating to the IMU and is injected, by the Allegro, into the geophysical data stream with a timestamp. In post processing, the software correlates the timestamps between the Allegro data and the IMU data and then provides relative time offsets for samples based on Allegro times. This time correlation between the Allegro and the IMU is where the most significant timing errors occur because of cumulative and variable latencies within the Allegro and EM-61. It is estimated that these timing errors currently contribute as much as a few centimeters of position error under normal operating velocities of less than a meter per second. Quantifying these timing errors proved to be difficult; mitigating these timing errors by replacing the Allegro data collection unit is an easier solution and will be a primary focus for the development of the next generation of SAINT.

3. Demonstration Design

3.1 Performance Objectives

The performance objectives of SAINT are summarized below in Table 3.

Type of Performance Objective	Primary Performance Criteria	Expected Performance (Metric)
Quantitative	Location accuracy	≤ 2 cm (1 σ)
	Survey rate for 2m x 2m area	≤ 5 min
	Post-processing time for 2m x 2m area	≤ 5 min
	Setup time (once per day)	≤ 5 min
	Density of coverage	EM sensor data on 10 cm or less increments
	ZUPT time	≤ 30 sec
	Free navigation time	≥ 30 sec
	Total "on" time before CF download or batteries needed	2 hours
Qualitative	System easy to setup and calibrate by a two person team	Yes or No
	System easy to operate by a two person team	Yes or No
	Post processing software easy to operate by inexperienced user	Yes or No

Table 3: Performance Objectives

The location accuracy objective of <= 2 cm (1 σ) is a relative error. Location accuracy was assessed using the pen test method described in Section 3.4. In addition to this evaluation, the Arcsecond system, a laser-based 3D positioning system with cm-level positioning error, was used as an independent ground truth system to establish location accuracy. SAIC (formerly AETC) conducted the Arcsecond testing. The results of this comparison are documented in Appendix E of this report.

Within the dynamic range of the IMU, location accuracy is not highly correlated to the dynamics of motion. The primary source of position errors are the IMU sensor errors, gyro and accelerometer white noise and biases (which change every time the unit is powered on), that are integrated into position errors over the free navigation interval. An additional source of position error is created by the time-tagging between the IMU data and the EM61-HH (latency between sensor and position data). Faster motion magnifies the impact of latency errors and slower motion minimizes the impact of these errors. Position errors are sensitive to the duration of motion: longer periods of free navigation have greater errors and shorter durations have lesser errors. Theoretically, the largest position errors should occur halfway through the free

navigation period since the R-T-S Smoother constrains the errors at the start and end of the free navigation period when the IMU is placed on the tripod.

3.2 Selecting Test Site(s)

The criteria for selecting a test site were the following:

1. Accessible to all project participants.
2. Buried metallic targets that can be used to compare sensor data both with and without the presence of SAINT.
3. A controlled site with locations of items known so that it may be revisited to gauge improvement and the geophysical data and positioning data may be compared to previous geophysical surveys and technologies.

The selected test site was the Aberdeen Proving Ground (APG) UXO calibration grid demonstration site. Common limiting factors of navigation equipment, such as vegetation and tree cover are not a factor at the calibration grid, but they do not affect SAINT's performance.

3.3 Test Site History/Characteristics

The Standardized UXO Sites Program has test methodologies, procedures, and facilities to help ensure that critical UXO technology performance parameters such as detection capability, false alarms, discrimination, reacquisition, and system efficiency are accurate and repeatable. The Aberdeen Proving Ground, MD site is a 17-acre complex composed of 5 independently scored scenarios. The scenarios include calibration area, blind grid, wooded, moguls, and open field. Within the open field there are a variety of challenges, which include electrical lines, gravel roads, fence line, wet areas, and clutter fields. All grids have been surveyed many times with multiple instruments including the EM61-HH.

This test utilized only the Calibration Area (#1), as shown in Figure 5. This area is seeded with inert OE items ranging in size from small (20 mm) to large 155 mm objects, 8 lb. and 12 lb. shotputs and loops of wire ranging in depth from .1m to 2.0 m. We interrogated 23 items that include 3 each of 20 mm, 40 mm, 57 mm, 60 mm, 81 mm, 2.75", 105 mm and 155 mm seeded items at different orientations/depths as well as one 8 lb. shotput. The items are in lanes 3 A, C, & D, 4 A, C,& D, 6 A, C & D, 7 A, C, D, H, J, & K, 8 A, C & D, 13 F & H, 14 F & H and Shotput lane 10G. These are the same items that were interrogated as in the previous demonstration with the addition of the smaller 20 mm and 40 mm items in lanes 3 and 4. These smaller items were added since the EM61-HH is more effective with smaller items than the G-858.

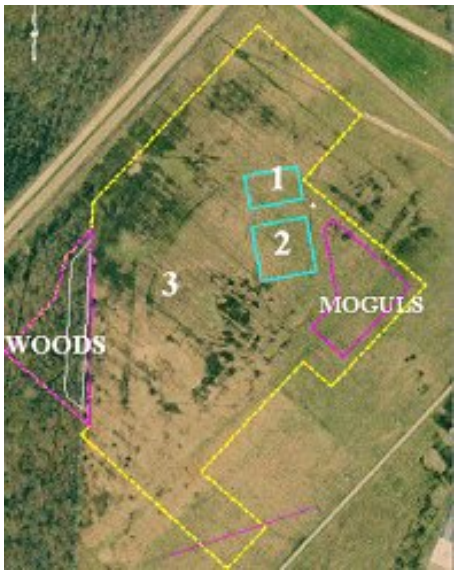

Figure 5: APG UXO demonstration site layout (#1-Calibration area)

3.4 Present Operations

The APG UXO Demonstration Site is maintained to provide quantitative, benchmarked evaluation of sensors and DGM systems and components.

3.5 Pre-Demonstration Testing and Analysis

Testing was performed at ENSCO prior to the demonstration at APG to quantify position accuracy. In addition to the estimate of position errors provided by the Kalman filter and R-T-S Smoother in the state covariance matrix, P, a straightforward "pen-test" method was developed to independently estimate position errors and to validate error estimates reported by the R-T-S Smoother as described below. The relative location accuracy objective for the project was <= 2 cm (one standard deviation) as shown in Table 3.

The pen-test is a simple means to precisely determine the position accuracy of the SAINT system. A felt-tip marker ("Sharpie") is rigidly attached to a calibration bracket that is temporarily mounted to the EM61 coil as shown in Figure 6. The operator moves the device, allowing the pen to draw a path along a large sheet of paper. By comparing the actual position that the device was moved over (as recorded by the drawing on the paper) with the computed position from the SAINT system, we can evaluate the accuracy of SAINT. Two-dimensional tracking verification is accomplished by constraining the free-navigation to a single plane.

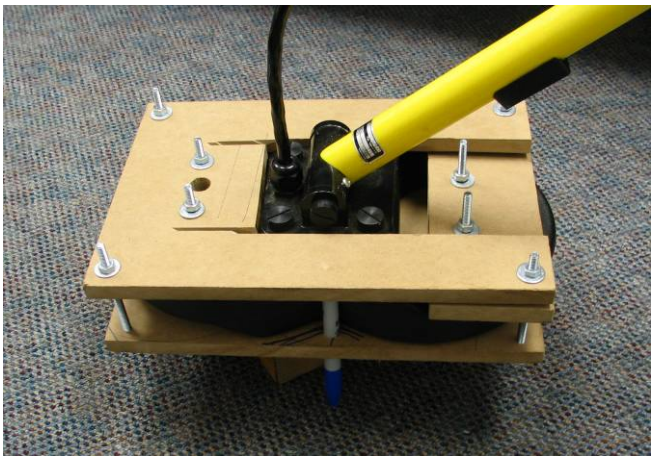

Figure 6: A "Sharpie" marker was rigidly mounted to the EM61 coils for this test.

This test was designed to evaluate errors in the inertial position estimates. Several errors are inherent to this validation test:

- "Sharpie" location: The precise location of the "Sharpie" tip relative to the center of navigation in the IMU (in the body-frame of the IMU) was measured based on the mechanical design drawings. This relative position is estimated to induce errors of up to 0.5 cm.
- Flexure in the "Sharpie" pen tip: The pen tip is flexible and can move relative to the mount on the EM61 coil. It is estimated that flexure in the pen tip might induce errors of up to 0.5 cm.
- Paper stretch and rectification: The paper the pen-test draws on can stretch; the image is digitally scanned for processing. Each phenomenon is expected to induce errors of up to 0.1 cm.

Data Collection

The pen-test data acquisition consisted of the following four steps.

- A large (6'x3') sheet of white paper was placed on a level, horizontal ground surface. A scale was drawn on the paper.
- Initial ZUPT: The unit was set down on a tripod mount with the EM61 coil stationary on the sheet of paper for 15 seconds.
- The operator picked up the unit and drew a path on the paper using the pen. This took approximately 30 seconds.
- Final ZUPT: Operator returned the unit to its original location on the tripod with the EM61 coil in its original location on the paper for a final "zero calibration" for about 15 seconds.

Processing

The drawing that results from the survey was optically scanned. The SAINT IMU data was post-processed through a Kalman Filter and R-T-S Smoother. The position of the pen tip, whose position offset to the IMU was measured in the lab, was then calculated based on the attitude and position of the IMU. Common points on the drawn "Sharpie" path (scaled to meters based on scale drawn on the paper) and the IMU estimated "Sharpie" path were selected and passed into

least-squares routine that rotates and translates the estimated path to be overlaid on the drawn "Sharpie" path.

Pre-demonstration Test

A superimposed data set based on a test of the method prior to the APG demonstration is shown in Figure 7. The black line represents the drawn "Sharpie" path, and the red line represents the path estimated using the R-T-S Smoother. The blue ellipses correlate to the 95% confidence errors estimated by post-processing software and are plotted roughly every 0.5 seconds. The collection speed for this data acquisition ranged from 25 cm/s when turning corners to 80 cm/s during the long passes as shown in Figure 8.

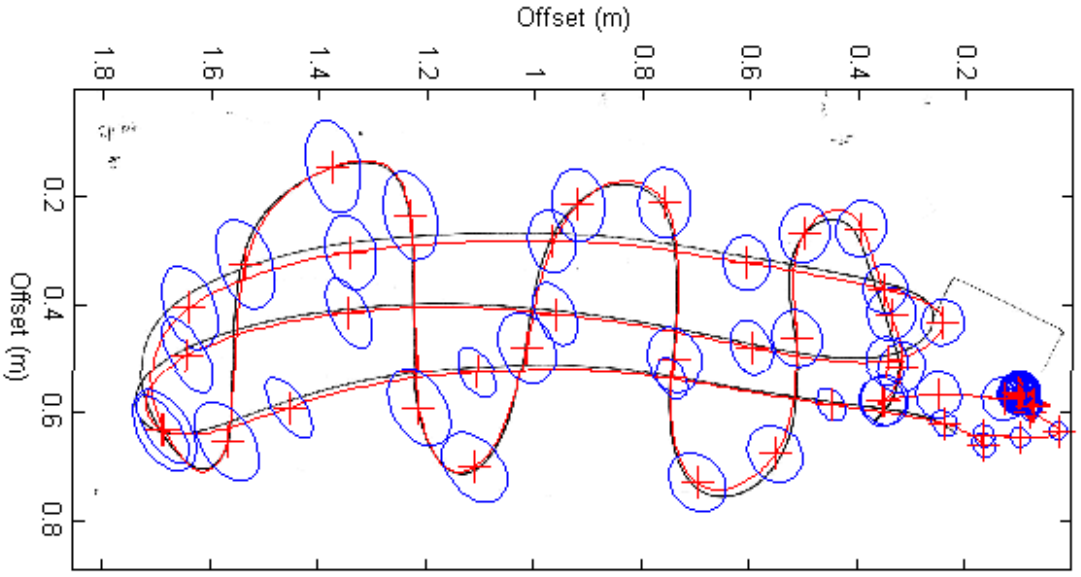

Figure 7: The black line represents the actual path, and the red line represents the path estimated using the R-T-S Smoother. The blue ellipses correlate to the 95% confidence errors estimated by post-processing software.

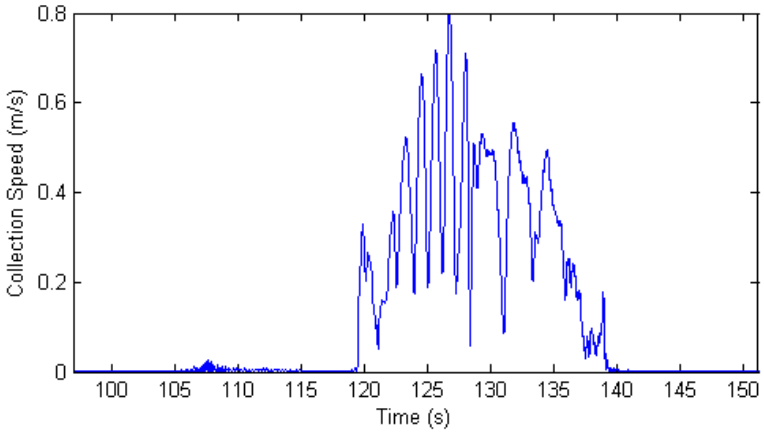

Figure 8: Data were acquired at collection speeds ranging from 0.25 m/s when turning corners to a maximum speed of 0.80 m/s, with an average speed of 0.38 m/s.

Position errors in the R-T-S Smoother path estimate relative to the drawn path were computed for each of the three axes, where the long axis in Figure 7 was defined as the y-axis, the short axis as the x-axis and the z-axis to be up (left-handed coordinate frame). Since it is not possible to correlate positions in time for the two paths the correlation was performed using a best fit between points in the drawn plot and computed plot. Horizontal errors (x-axis and y-axis) were computed from the differences in position between the points on the drawn path and the nearest point on the computed, best fit path. The horizontal errors were estimated at each of the error ellipses shown in Figure 7. The vertical errors (z-axis) were computed as the difference from the vertical position mean under assumption that the paper was placed on a level surface.

The plot in Figure 9 shows the measured errors for the x-axis (solid red line) and y-axis (solid blue line) and their corresponding error bounds (2 standard deviations) as output by the R-T-S Smoother.

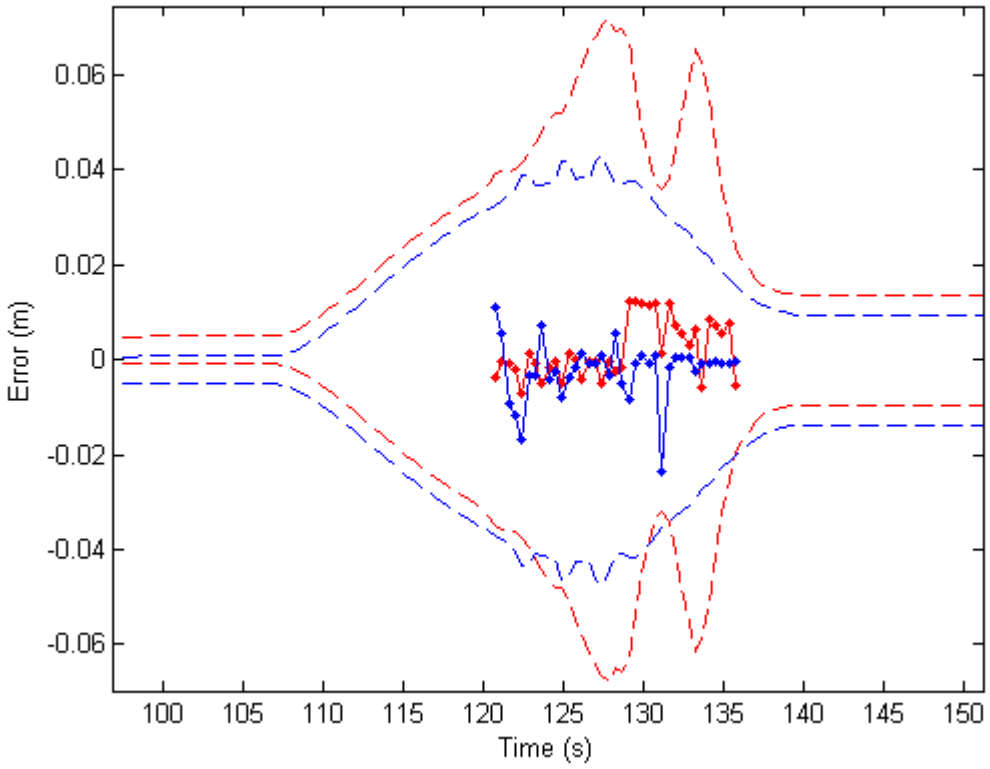

Figure 9: Position errors during free navigation interval (solid red line = x-axis position error, dashed red lines = R-T-S Smoother 2 standard deviation x-axis error bounds, solid blue line = y-axis errors, dashed blue lines = R-T-S Smoother 2 standard deviation y-axis error bounds)

The plot in Figure 10 shows the measured errors for the z-axis (solid black line) and the corresponding error bounds (2 standard deviations) as output by the R-T-S Smoother.

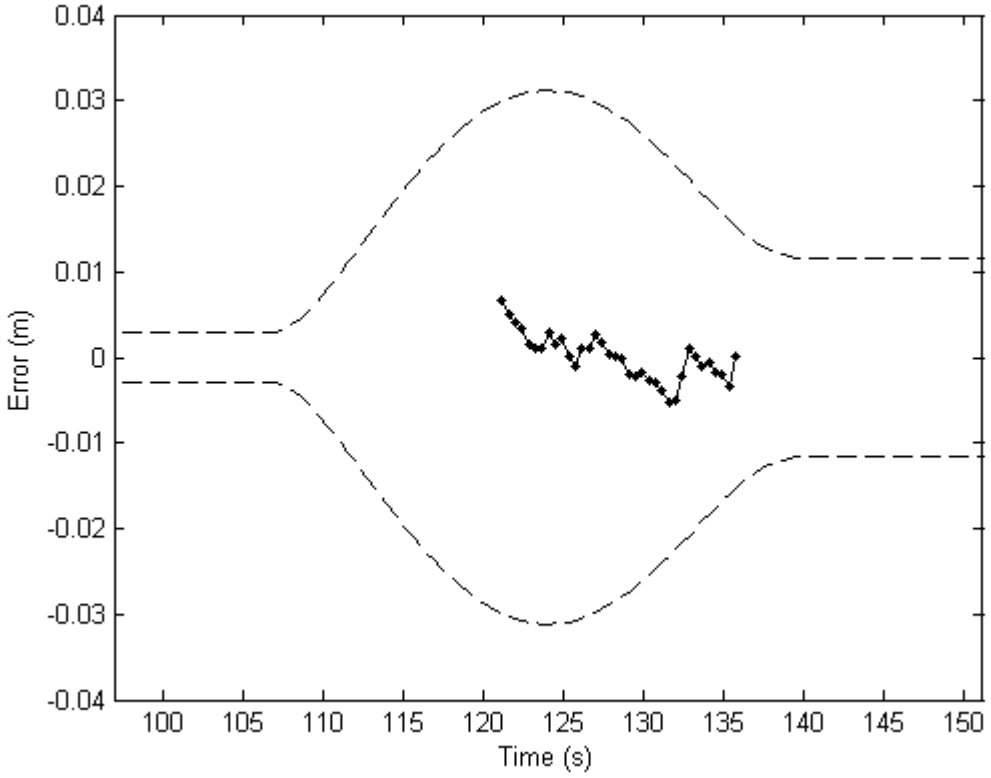

Figure 10: Z-axis position errors during free navigation interval (solid black line = z-axis position error, dashed black lines = R-T-S Smoother 2 standard deviation z-axis error bounds)

A summary of the maximum, mean and standard deviation in the location errors based on the pre-demonstration test is provided in Table 4.

	Max Error (m)	Mean Error (m)	Standard Deviation Error (m)
X	0.012	0.002	0.006
Y	0.011	-0.002	0.006
Z	0.007	0.000	0.003

Table 4: Summary of position errors

The reported position errors are based on the pen test method error analysis. The Arcsecond error analysis performed by SAIC (formerly AETC, Inc.) is provided in Appendix E and concludes that the radial errors ranged from 1-3 cm using Arcsecond as ground truth for the majority of the data sets and roughly 1 cm radial error using model-based electromagnetic inversion fits.

3.6 Testing and Evaluation Plan

3.6.1 Demonstration Set-Up and Start-Up

The demonstration setup involves attaching SAINT to the EM61-HH, which includes the following:

- Attach SAINT to the EM61-HH shaft using the shaft clamp. See Figure 11.
- Lock the hinge of the EM61-HH using custom bracket (tie-straps and shaft clamp). See Figure 12.
- Connect data cable from SAINT to EM61-HH data hub (Allegro CE).
- Connect power cable from battery pack to SAINT. Turn "on" the power switch.
- Measure the offset between the EM61-HH sensor head and the inertial sensor of SAINT in the body frame of the inertial sensor.

Once powered "on," SAINT begins recording IMU and DMC data and will continue collection until the unit is powered "off." All data is stored on a compact flash (CF) card, which can downloaded once at the conclusion of collection or alternatively downloaded via serial port transfer.

Operation is intended for a single operator in possession of the SAINT-metal detector system. During field collections it can be helpful for a second operator to monitor the performance of the first, record notes about the survey, and provide relief when necessary.

Figure 11. SAINT attached to the EM-61 HH handle.

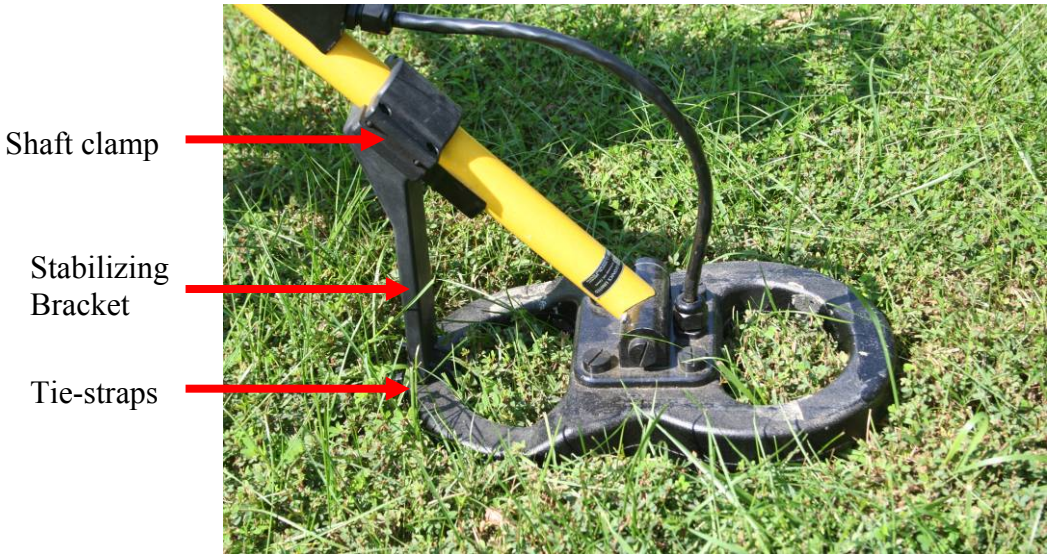

Figure 12: Hinge locking mechanism for EM61-HH

Download

For serial download, connect the USB/serial cable to a computer and set the computer to receive and record the data. Then, power on the SAINT system. The system will detect that there is a USB/serial cable connected and initiate transfer of data. Serial data transfer occurs in a series of short bursts. Each burst happens at 115200 bps, and the primary driver of the overall data rate is the period between bursts. It takes several hours to download a 1 hour collection because the effective data rate is approximately 1 kilobyte / second.

Due to the slow data rate the current preferred method for extracting inertial data from the unit is to open the case and extract the CF card. This process is complicated due to the initial case design and board design not intending to promote CF card extraction. To remedy this we intend to redesign the adapter card to include an ATA header, and add a daughter card that contains the CF card mount. Additionally, we propose creating a slot in the face of the handle, and adding a "door" with a seal to prevent moisture intrusion into the electronics enclosure.

3.6.2 Period of Operation

ENSCO's demonstration at APG occurred on September 12-13, 2006. Minor errors in the data acquired on the first day limited its use in demonstrating the system performance. On the second day, in addition to data acquisition over 23 targets in the calibration lane and a test to determine the effect of SAINT on the EM61, a pen test and an Arcsecond test were performed at the beginning and end of the day.

3.6.3 Area Characterized or Remediated

This test utilized only the Calibration Area (#1), as shown in Figure 5. This area is seeded with inert OE items ranging in size from small (20 mm) to large 155 mm objects, 8# and 12# shotputs and loops of wire ranging in depth from .1m to 2.0 m. We interrogated 23 items that include 3 each of 20 mm, 40 mm, 57 mm, 60 mm, 81 mm, 2.75", 105 mm and 155 mm seeded items at different orientations/depths as well as one 8# shotput. The items are in lanes 3 A, C, & D, 4 A,

C,& D, 6 A, C & D, 7 A, C, D, H, J, & K, 8 A, C & D, 13 F & H, 14 F & H and Shotput lane 10 G.

3.6.4 Residuals Handling

This section is not applicable.

3.6.5 Operating Parameters for the Technology

All operating parameters are fixed during standard operation. The only requirement is for the operator to follow the routine procedure.

The desired coverage density of sensor data within the interrogation area limits the speed at which the device should be swept over the area. Since sensor data is collected at discrete time intervals, desired sensor data density along the path over which the sensor is swept can be obtained by regulating the speed at which the sensor is swept. Free navigation is limited to 30 seconds to minimize positioning error. To cover a larger area than can be swept in 30 seconds, two or more data sweeps must be performed in series (separated by a ZUPT). A sample sweep pattern is shown in Figure 13. Since the ZUPT locations are the same, no special operation has to be performed in the post-processing software to overlay the adjacent collections.

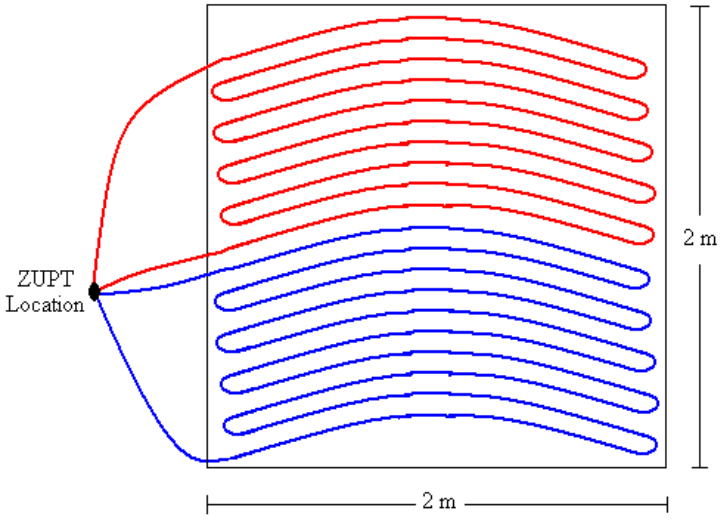

Figure 13: Sample sweep pattern to cover a 4 m^2 area in two passes.

The following tests were performed to validate performance objectives as outlined in Table 3.

Calibration Prior to Testing

There is a position offset from the IMU to the EM61-HH sensor that must be computed each time the IMU is mounted to a different location on the EM61-HH staff. Although this offset is currently measured in the lab, calibration data were acquired at the beginning of the day to test a Kalman filter algorithm under development (not part of this effort) to estimate this position offset.

The calibration procedure estimates the relative 3D position offset of the IMU to the pivot point, the center of the horizontal screw connecting the EM61-HH sensor head to the attached pole, and then we translate that position to the center of sensitivity of the EM-61. The center of sensitivity is located approximately 5 cm beneath the center of this screw when the coils are horizontal (note that we rigidly fix the pole orientation to the coil). This calibration procedure consists of keeping the pivot stationary while pitching and yawing through 180 degrees of motion over 10 seconds and then returning the IMU to its starting location. Since the IMU measures both three-dimensional position and attitude, it is only necessary that this pivot point does not move (rotate or translate) relative to the IMU while you pitch, yaw and translate the IMU.

Pen test Method

The pen-test method was performed twice during the APG demonstration to provide redundant data for self-evaluation of the location accuracy. The tests were performed at the start and end of the day to determine if environmental changes (solar heating, battery discharge, etc…) impacted the location accuracy. The only difference in the performance assessment for the APG tests and the pre-demonstration tests is that the compass (integrated with the IMU) had been calibrated for the APG tests and provided a constraint to the IMU heading.

Arcsecond Test

The Arcsecond system was operated by SAIC (formerly AETC, Inc.) working under SERDP project MM 1381 as a ground truth system for a secondary evaluation of location accuracy. A special bracket was developed to mount the Arcsecond triad directly onto the EM61-HH shaft as shown in Figure 14. The tests were performed at the start and end of the day to determine if environmental changes (solar heating, battery discharge, etc…) impacted the location accuracy. A detailed description of the analysis can be found in Appendix E. The Arcsecond error analysis performed by SAIC (formerly AETC, Inc.) concluded that "typically, agreement between the two systems was found to be good to within 1-3 cm. The fit qualities with each positioning system were consistent with a < 1 cm positioning accuracy with the Arcsecond positioning giving noticeably better results."

Figure 14: Arcsecond system and SAINT mounted on EM61-HH at APG demonstration.

Collections

Geophysical data were collected in 3 successive passes over each of the 23 selected targets in the calibration grid with the integrated SAINT and EM61-HH system. SAINT position data are in an arbitrary, local level reference frame by default. However, for archival and comparison purposes to other activities, position data from the demonstration were transformed to UTM based on the known coordinates where the IMU was located during a ZUPT. When the data were processed, the resulting position data and geophysical data were automatically saved to a separate tab-delimited text file for each pass over each of the 23 targets.

Effects Test

To evaluate the impact on EM61-HH data on the operation of SAINT, EM61-HH data was collected with the SAINT system turned on and turned off over a target while stationary. Because the relative location of the IMU to the EM61-HH sensors coils is static, the impact of the SAINT hardware on the EM61-HH data will be a static bias due to the presence of metal (primarily the IMU) within the field of the sensor. Since the EM61-HH is an uncalibrated sensor with a user-adjustable bias adjustment, the user can either manually adjust the bias in the field or in software to remove this effect. There is a theoretical possibility of tertiary induced fields affecting the sensor (the secondary fields induced in a target then inducing tertiary fields in the SAINT hardware, that are then measured by the sensor), but the amplitude of this phenomenon is presumed to be negligible. A statistical comparison of the variance in the EM61-HH data during times when SAINT is turned off to times when SAINT is turned on showed that the variance in the recorded EM61-HH data was the same to better than 95% confidence (using Levene's test) whether the unit was turned on or off (see 4.3).

Figure 15: Data collection over geophysical target at APG demonstration.

3.6.6 Demobilization

Demobilization requires disconnecting SAINT from EM61-HH, repacking the equipment in shipping cases, and departing the site. There should be no lasting impact to the site from this demonstration.

3.7 Selection of Analytical/Testing Methods

This section is not applicable.

3.8 Selection of Analytical/Testing Laboratory

This section is not applicable.

4. Performance Assessment

4.1 Performance Criteria

The primary performance criteria for this project are stated in Table 3. The successful demonstration of the SAINT technology at APG essentially consisted of collecting an adequate density of EM61-HH geophysical data (<= 10 cm between samples) while maintaining a relative location accuracy <= 2 cm (one standard deviation). Secondary demonstration objectives were to show robustness and reliability of the system, efficient data acquisition, ease of use, and simplicity of post-processing. The post-processing software was not demonstrated at the time of the demonstration but was later validated at ENSCO by CEHNC and SAIC (formerly AETC) on February 6, 2007.

The utility of this precision position data integrated with the EM61-HH sensor for target characterization was beyond the scope of the demonstration and will be established by other researchers. Data has been provided to interested researchers and specifically to AETC, Inc. working under SERDP MM 1381.

4.2 Performance Confirmation Methods

Most of the quantitative objectives consisted of either acquisition or processing times and were simply confirmed based on acquisition times written in field notes and timing of the post-processing software.

ENSCO's pen-test method described in Section 3.5 was the primary method for establishing the location accuracy demonstrated at APG. The error analysis for determining location accuracy using Arcsecond data as ground truth is described in Appendix E.

4.3 Data Analysis, Interpretation, and Evaluation

Post-processing includes a Kalman filter and R-T-S smoother to optimally estimate the IMU position and transform the IMU estimated positions to sensor positions, and also consists of the merge of EM61 and position data. The post-processing is mostly automatic, requiring only the selection of data files and the periods to process. The error estimates output from the post-processing software were validated by comparison with the independent assessment of errors based on the pen-test method described in Section 3.4.

Plots of the processed position data overlain on the pen path for the start-of-day and end-of-day tests are shown in Figure 16 and Figure 18, respectively. The corresponding location errors are shown in Figure 17 and Figure 19, respectively. For the pre-demonstration testing, the lack of a calibrated compass during testing resulted in large heading uncertainties in the R-T-S Smoother; these heading uncertainties induced the local oscillations in the R-T-S position error bounds in the pre-demonstration test. For the APG tests, the improved heading accuracy based on the use of the compass data significantly reduced the position error estimates provided by the R-T-S Smoother algorithm, such that the x-axis and y-axis error bounds in are nearly co-aligned and indistinguishable in Figure 17 and Figure 19.

APG Test #1- Collected at start of day

Plots of the processed position data overlain on the pen path for the start-of-day and end-of-day tests are shown in Figure 16. The corresponding location errors are shown in Figure 17.

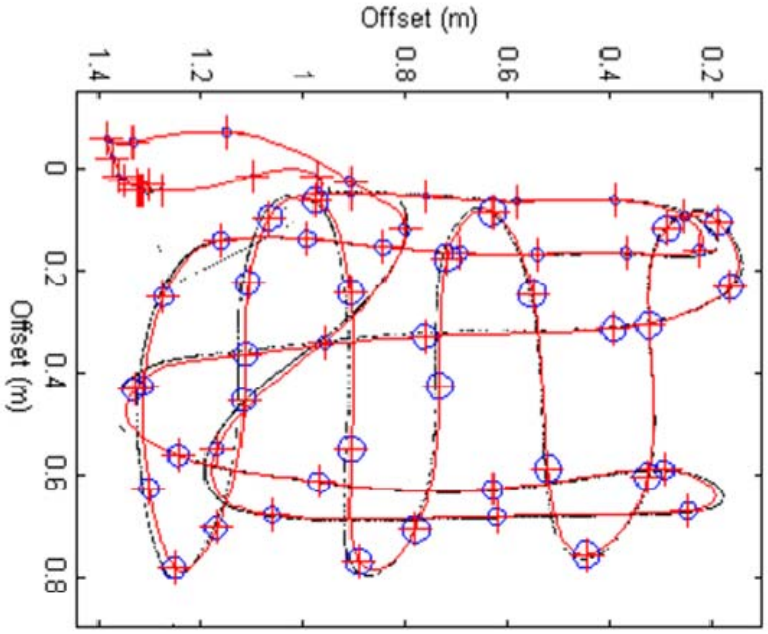

Figure 16: The black line represents the actual path, and the red line represents the path estimated using the R-T-S Smoother. The blue ellipses correlate to the 95% confidence errors estimated by post-processing software.

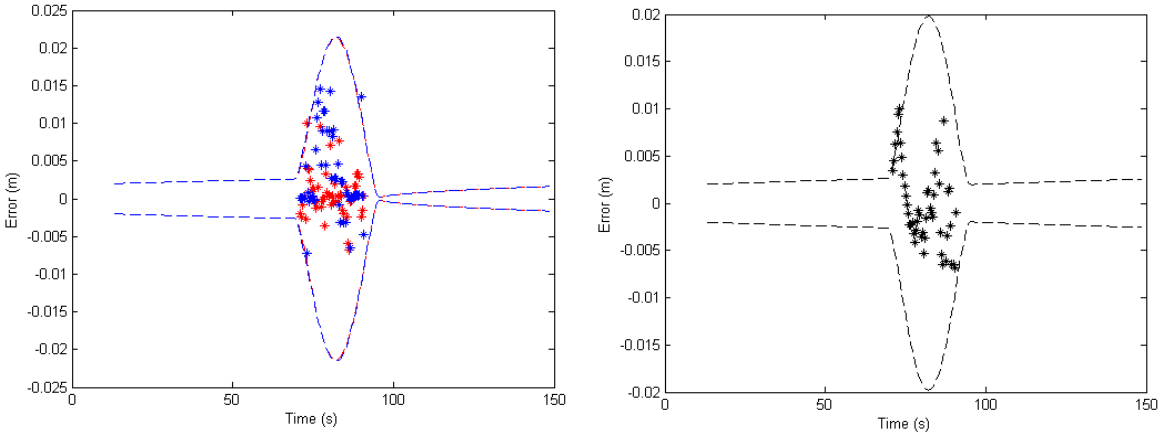

Figure 17: Position errors during the free navigation interval (red asterisks = x-axis position error, dashed red lines = R-T-S Smoother 2 standard deviation x-axis error bounds, blue asterisks = y-axis errors, dashed blue lines = R-T-S Smoother 2 standard deviation y-axis error bounds, black asterisks = z-axis position error, dashed black lines = R-T-S Smoother 2 standard deviation z-axis error bounds)

A summary of the maximum, mean and standard deviation in the location errors for the start-of-day are provided in Table 5.

	Max Error (m)	Mean Error (m)	Standard Deviation Error (m)
X	0.010	0.001	0.003
Y	0.015	0.003	0.005
Z	0.010	0.000	0.004

Table 5: Summary of position errors – APG #1

APG Test #2 – collected at end of day

Plots of the processed position data overlain on the pen path for the start-of-day and end-of-day tests are shown in Figure 18. The corresponding location errors are shown in Figure 19.

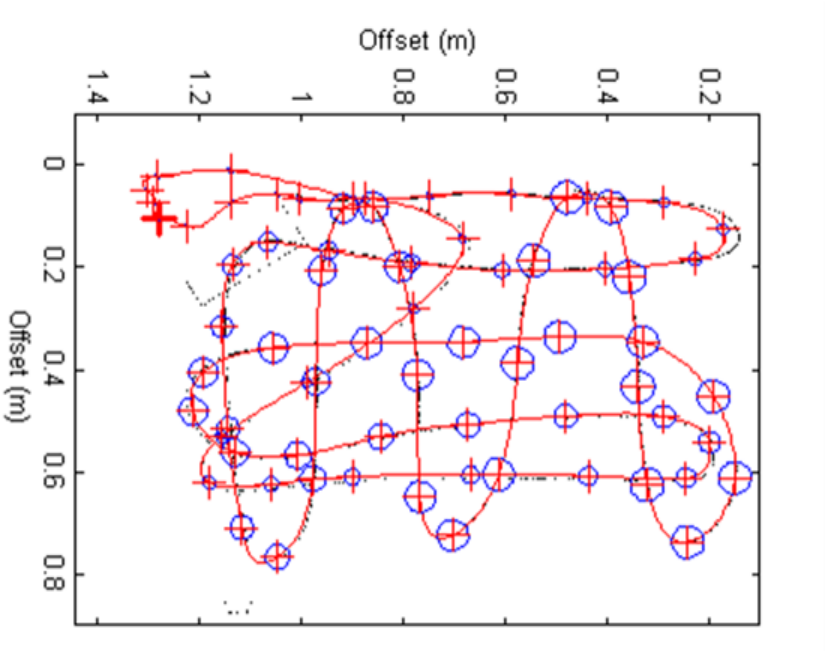

Figure 18: The black line represents the actual path, and the red line represents the path estimated using the R-T-S Smoother. The blue ellipses correlate to the 95% confidence errors estimated by post-processing software.

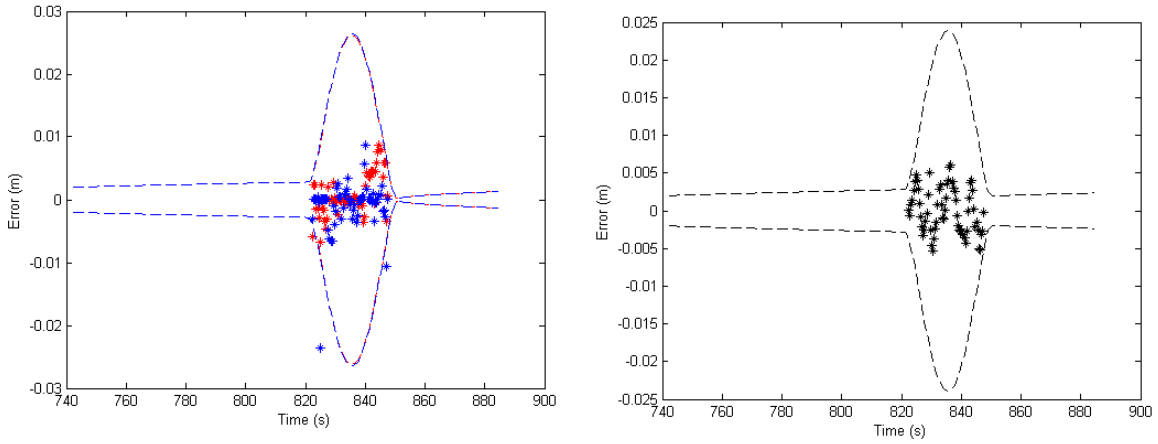

Figure 19: Position errors during the free navigation interval (red asterisks = x-axis position error, dashed red lines = R-T-S Smoother 2 standard deviation x-axis error bounds, blue asterisks = y-axis errors, dashed blue lines = R-T-S Smoother 2 standard deviation y-axis error bounds, black asterisks = z-axis position error, dashed black lines = R-T-S Smoother 2 standard deviation z-axis error bounds)

A summary of the maximum, mean and standard deviation in the location errors for the end-of-day tests are provided in Table 6.

	Max Error (m)	Mean Error (m)	Standard Deviation Error (m)
X	0.009	0.001	0.003
Y	0.024	-0.001	0.004
Z	0.006	0.000	0.003

Table 6: Summary of position errors – APG Test #2

Based on the analysis of location errors using the pen-test method, the standard deviations in position error for all three axes were well below the project objective of 2 cm (one standard deviation) as shown in Table 7.

	Pre-demonstration	APG #1	APG #2
X	0.006	0.003	0.003
Y	0.006	0.005	0.004
Z	0.003	0.004	0.003

Table 7: Summary of standard deviation in position errors for pre-demonstration and APG tests.

These tests show that the location errors are within the two standard deviation bounds of the R-T-S Smoother estimates.

Density of coverage

The linear density of geophysical data coverage was confirmed by computing the incremental distances between EM61 data for all of the processed data from the 23 sites. The incremental

distance between EM61 data never exceeded the project objective of 10 cm while collecting data over the sites as can be seen in Figure 20. The density of geophysical data is limited by the maximum data acquisition rate of 15 Hz of the EM61-HH.

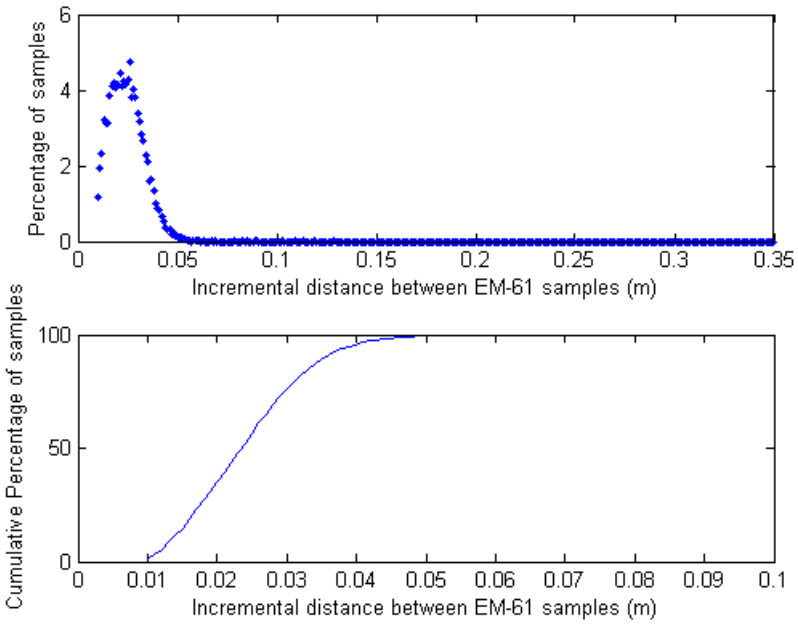

Figure 20: The top plot is a histogram showing the distribution of the incremental distances between EM61 data samples. The bottom plot shows that 100% of the data were collected with incremental distances of less than 5 cm.

SAINT effect on EM61-HH

Because the EM61-HH sensor is directional and SAINT is positioned off the coil axis in the operational configuration, it should be expected that the effect is small. Furthermore, by using a MEMS IMU and only digital logic circuitry the SAINT has neither large moving parts nor large currents to create fields measurable by the EM61-HH.

In order to determine the effect of running SAINT near the EM61-HH on the metal detector readings, data were collected for approximately 3 minutes during which SAINT was turned on and off several times. SAINT was in its operational configuration and left stationary during the entire test. Figure 21 shows the data collected on each channel and the start of the turn on and turn off times for the SAINT system marked in green and red, respectively.

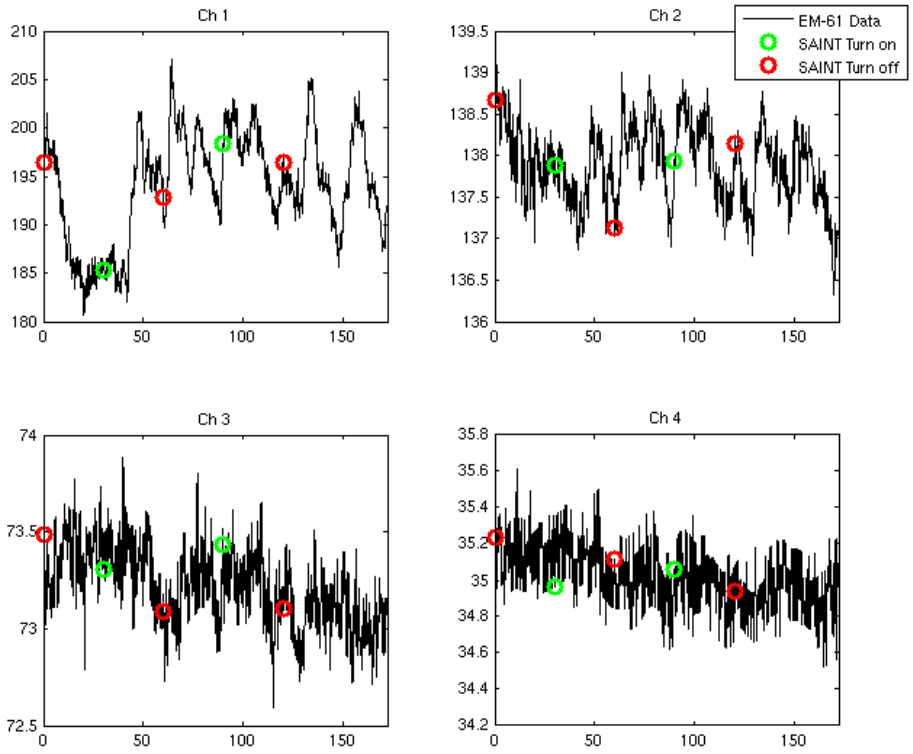

Figure 21: EM61-HH data from all four channels of the EM61-HH MK2. Red circles indicate when the instrument was turned off; green circles indicate when the instrument was turned on. Thus the status of SAINT for any data point is reflected in the color of the nearest circle to the left.

First, notice that on channels 2, 3, and 4 the reading variances are much less than the sample means (less than 0.2% for those channels). This indicates that if SAINT has any affect on the data from channels 2, 3, or 4 it is at most very small. While channel 1 data has a large variance, correlated errors in the data do not correspond to SAINT turn on / turn off times.

No correlation between the SAINT status and EM61-HH data is obvious in the plotted data. Levene's Test, a statistical method to determine if two groups of samples have equal variances, was used to test for changes in the data corresponding to SAINT turn on/off. The data in figure 1 were separated into two groups identified by power status of the SAINT (on or off). The computations were performed for each channel.

By Levene's test the EM61-HH data has the same variance to better than 95% confidence whether the SAINT is turned on or off. Consequently, it is unlikely that the power status of the SAINT has any significant effect on EM61-HH system noise.

All of the positions in the delivered geophysical data have been transformed to UTM. We were provided with the UTM coordinates of our four ZUPT locations and the geophysical targets using conventional surveying techniques. Since the output positions of the SAINT post-processing software are in a local frame oriented to true north with the origin at the ZUPT

location, the output positions were simply translated to such that the coordinates of the origin matched the surveyed ZUPT coordinates. Since the surveyed geophysical targets are also in the UTM frame, a plot of SAINT's output coordinates should overlay the coordinates of the geophysical targets as shown in Figure 22. However, this is not the case for two of the four ZUPT locations; differences between the surveyed geophysical targets and SAINT's output coordinates differ by greater than a meter. After re-surveying the ZUPT locations and repeatably demonstrating the location accuracy of SAINT when collecting data over distances greater than five meters, two additional potential causes of these errors are inaccurate field notes or the disturbance of the IMU during the ZUPT phase. Studies of the sensitivity analysis of the disturbance of the IMU during the ZUPT phase will be part of future development efforts.

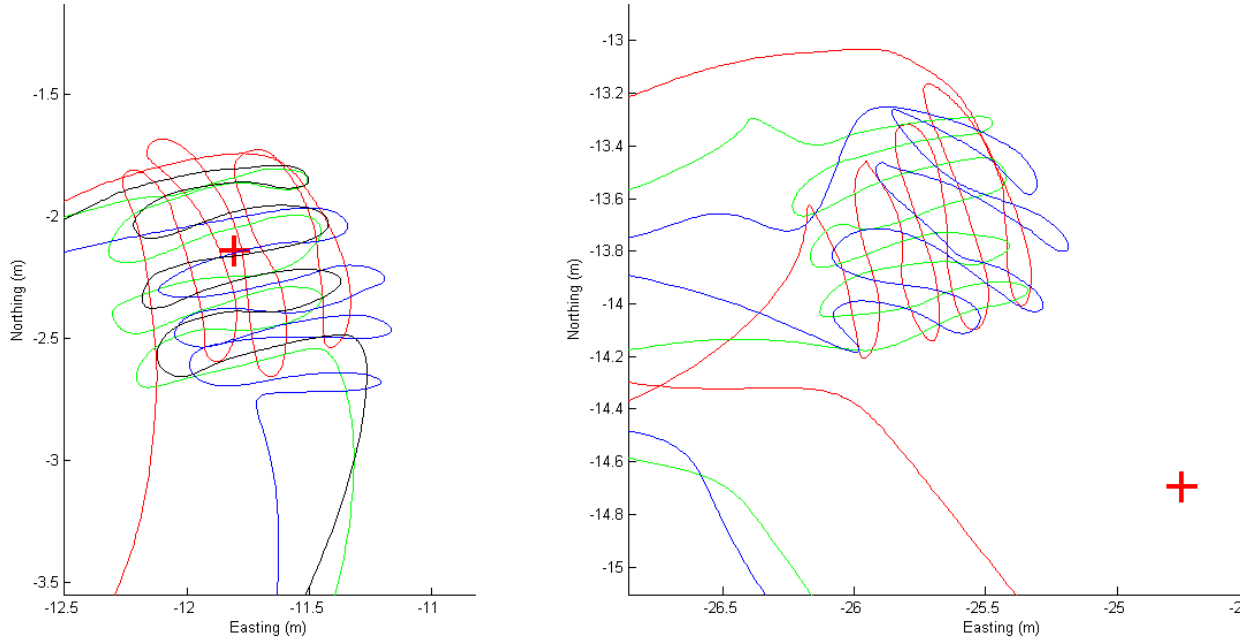

Figure 22: The figure on the left shows the relative position of the EM61-HH sensor for four data collections over cell A7 with a red plus denoting the surveyed location of the geophysical target. The plot on the right shows the relative position of the EM61-HH sensor for three data collections over cell F13 with a red plus denoting the surveyed location of the geophysical target.

Self-Evaluation

The SAINT system exceeded the project objective for location accuracy of 2 cm by a factor of four in both pre-demonstration testing and at the demonstration. The primary sources of location errors are the gyro and accelerometer biases. These biases change every time the unit is turned on and hence, cannot be simply estimated once and removed from the data but must be continually estimated inside the Kalman filter. The use of zero-velocity updates and position updates (when the unit is returned to the ZUPT stand after each free navigation period) enable the Kalman filter and R-T-S Smoother to estimate and remove these biases. These biases limit the length of free navigation time for collecting data.

A summary of ENSCO's self-evaluation is included in Table 8. Most of the quantitative objectives consisted of either acquisition or processing times and were simply confirmed based on acquisition times written in field notes and timing of the post-processing software.

Type of Performance Objective	Primary Performance Criteria	Expected Performance (Metric)	Actual Performance
Quantitative	Location accuracy	≤ 2 cm (1 σ)	3-5 mm
	Survey rate for 2m x 2m area	≤ 5 min	4.3 min
	Post-processing time for 2m x 2m area	≤ 5 min	3.25 min
	Setup time (once per day)	≤ 5 min	< 5 minutes
	Density of coverage	EM sensor data on 10 cm or less increments	100% coverage <= 10 cm increments
	ZUPT time	≤ 30 sec	17 sec
	Free navigation time	≥ 30 sec	28 sec
	Total "on" time before CF download or batteries needed	2 hours	4 hours
Qualitative	System easy to setup and calibrate by a two person team	Yes or No	Yes
	System easy to operate by a two person team	Yes or No	Yes
	Post processing software easy to operate by inexperienced user	Yes or No	Demonstrated 2/07/2007

Table 8: Self-evaluation of performance objectives

The location accuracy was independently evaluated by SAIC (formerly AETC, Inc.) using the Arcsecond system as ground truth as described in Appendix E. The evaluation concluded that the majority of the acquired Arcsecond and SAINT sensor position data showed agreement to within one to three centimeters. However, for two of the trials, the SAINT trajectory drifted way off relative to the Arcsecond data. ENSCO has been unable to duplicate the problem seen with the last two trials of the field test during subsequent testing. We can see no obvious answer for these errors in the data set. Hardware stabilization and continued field testing in the next Phase of this program may help determine the cause of this problem. Analysis of the EM61-HH data merged with SAINT's position data using model-based EM inversion fits is also described in Appendix E and concluded that radial position errors were less than 1 cm.

In addition to the demonstrated location accuracy, the system was shown to be easy to setup and operate and met the project objectives for survey rates and post-processing times, which lead to efficient field operations. No measurement of the actual time to set up the system was documented during the demonstration, but the system routinely took less than 5 minutes to set up

during testing. The free navigation time was calculated as the average time during which the IMU was moving (start and stop times were extracted from the accelerometer data) for all 23 of the targets interrogated. The average time of 28 seconds is slightly lower than the objective of 30 seconds because the operator was returning the system to the ZUPT location when cued by the audible warning signals that the 30 seconds of free navigation was approaching.

Position and sensor data were made available to AETC, Inc. working under SERDP project MM 1381 and will be delivered with this report for other researchers interested in the characterization problem.

5. Cost Assessment

5.1 Cost Reporting

The SAINT technology is directed toward allowing more effective selection of which detected targets underground should be excavated at OE sites. Since excavating non-hazardous objects can represent the majority of OE remediation expenses, the potential impact of this technology is significant.

There are three primary cost factors associated with SAINT and its impact of OE remediation: 1) the cost of the system, 2) the production rate (how fast and efficiently it can be operated), and 3) the effectiveness of the derived target dig lists.

The cost of a commercial SAINT system has not been determined. However, the critical component of SAINT, the Honeywell HG1900 IMU, has the largest part cost of approximately $10,000 at the time of this writing. Market forces indicate that IMUs in this MEMS line of products should decrease to approximately $5000 per unit within 2-4 years. Other components of SAINT are much less costly. Therefore, the cost of a SAINT system is comparable to the cost of current geophysical sensor systems (EM-61, G858, etc.) or a commercial Robotic Total Station (RTS) system ($20-30K).

The production rate observed for SAINT operations at APG was approximately 4 hours for 23 targets for a single operator using a single system. Therefore a single operator could interrogate approximately 6 targets per hour.

No effort was made under this project to evaluate the effectiveness of the target characterization algorithms. SAINT is designed as a tool to allow for data to be collected efficiently for target characterization; evaluation of the efficacy of these efforts is beyond the scope of this effort.

5.2 Cost Analysis

There is no existing technology which SAINT is designed to directly replace. However, setup time and costing is similar to the RTS. This is the closest technology commercially available that can come close to the INS accuracy. The RTS system has demonstrated an average accuracy of .07m (ref Millhouse: Innovative Navigation Systems to Support Digital Geophysical Mapping ESTCP #200129 Phase III APG Demonstration & Phase IV Development Draft Final Report 17-Feb-2006). In this report the Arcsecond system was demonstrated to provide an average accuracy of .01 m. However, the manufacturer of the system, Metric Inc (formerly Arcsecond), made a decision in February 2007 to discontinue development of the Arcsecond system

The cost impact of SAINT depends on the efficacy of target characterization efforts which are outside the scope of this effort. Therefore, the full impact of SAINT will not be known until the efficacy of characterization methods is better known.

Cost to operate SAINT consists of a single operator, employing a Geonics EM-61, integrated with the SAINT system. This operator can interrogate approximately 6 per hour, or 48 targets per day, at the production rate demonstrated. With experience and operating in a production setting, this rate is expected to double to 96 targets per day.

Given that an operator has been previously trained in using the EM-61 HH, SAINT specific hardware instruction could be accomplished in under two days. Improvements to hardware and software for ease of use in operational settings and system maintainability would reduce the instruction time to less than one day.

The primary cost driver to deploy SAINT is the production rate, which, given the EM-61 cost, SAINT cost, and labor cost, determines the interrogation cost per target. We can estimate this cost using the following rough order of magnitude estimates. Rental costs were taken from the web site of Exploration Instruments, www.expins.com:

Fully burdened daily labor cost (1 person)	$500
EM-61-HH daily rental cost	$60
SAINT daily rental cost (est.)	$100
PC daily rental cost	$20
Total daily cost	$680

At 96 targets per day, the average interrogation cost is therefore $7.08 per target. Life cycle costs are incorporated into the daily rental costs.

6. Implementation Issues

6.1 Environmental Checklist

There are no permits or regulations that impact this technology.

6.2 Other Regulatory Issues

There are no other regulatory issues.

6.3 End-User Issues

CEHNC is the lead on this project because of their pressing need for better technology for DGM and UXO operations. CEHNC is prepared to advocate and push this technology into the user community if it is shown to meet the objectives defined herein.

7. References

Rogers, R. M., 2000, *Applied Mathematics in Integrated Navigation Systems*, AIAA.

Rauch, H.E., Tung, F. and Streibel, C.T. (1965). "Maximum Likelihood Estimates of Linear Dynamic Systems", AIAA J, Vol 3, No., 8, pp. 1445-1450.

8. Points of Contact

Point of Contact	Address	Phone/Fax/Email	Role in Project
Scott Millhouse, PE	U.S. Army Corps of Engineers Engineering & Support Center-Huntsville 4820 University Square Huntsville, Alabama 35816-1822	Ph: 256-895-1607 Fax: 256-895-1737 scott.d.millhouse@ hnd01.usace.army.mil	Principle Investigator
David W.A. Taylor, PhD	ENSCO, Inc. 5400 Port Royal Rd Springfield, VA 22151	Ph: 336-632-1200 Fax: 336-632-1225 taylor.david@ ensco.com	Contractor Lead Scientist
Jane Bohlin	ENSCO, Inc. 5400 Port Royal Rd Springfield, VA 22151	Ph: 703-321-4681 Fax: 703-321-4609 bohlin.jane@ ensco.com	Contractor Task Manager

Signature of Project Lead

D. Scott Millhouse 16 July, 2007

Scott Millhouse, PE Date

APPENDICES

Appendix A: Analytical Methods Supporting the Experimental Design

Not required.

Appendix B: Validation Plan

Not required.

Appendix C: Quality Assurance Project Plan (QAPP)

C.1 Purpose and Scope of the Plan

The purpose of this plan is to outline the quality assurance procedures for this project.

C.2 Quality Assurance Responsibilities

QA Officer for this demonstration is Scott Millhouse, CEHNC. He will oversee the demonstration, assure compliance with the Work Plan, and attest to the results.

C.3 Data Quality Parameters

The most important aspect of quality assurance for this demonstration is that all measurements are accurately recorded and well documented. Detailed signed and dated field notes will accompany all digital data files. The QA officer will independently evaluate performance for the unknown areas of the grids and compare navigation accuracy and geophysical anomaly representations with past test results and the actual values and locations. A comparison matrix will be created showing field results as bench marked to the known locations.

C.4 Calibration Procedures, Quality Control Checks, and Corrective Action

TBD as required.

C.5 Demonstration Procedures

Demonstration procedures are described in the test plan. The only maintenance anticipated during the demonstration is exchange or recharging of batteries.

In addition to the demonstration procedures, digital photographs will be taken by a staff member of the Aberdeen Proving Grounds during conduct of the demonstration.

C.6 Calculation of Data Quality Indicators

Data quality for this demonstration primarily consists of accurate recording of data. The QA Officer will observe the recording of all data.

C.7 Performance and System Audits

All data will be reviewed at the end of each demonstration work day by the QA Officer with the demonstration team.

C.8 Quality Assurance Reports

The QA Officer will provide a final quality assurance report, primarily attesting to the correctness of the information acquired during the demonstration.

C.9 Data Format

All handwritten data and field notes will be written legibly, in ink, and signed and dated by the note-taker. Any entries that are corrected will be done with a single strike-through and will be initialed both by the note-taker and the QA Officer.

Most data collected during this demonstration will be digital and stored on computer disks in industry standard PC formats.

C.10 Data Storage and Archiving Procedures

Field notes will be recorded in data collection templates which will be scanned onto the computer disk for permanent storage with the data. Electronic data will initially be stored in the field on computer disks. Prior to leaving the field each day, all data will be copied onto CD-R disks for permanent storage. A copy will be provided daily to the QA officer.

Appendix D: Health and Safety Plan

This demonstration will be conducted in compliance with the existing Health and Safety Plan at the Aberdeen Proving Grounds, Maryland.

Appendix E: A Comparison of EMI Fits from Two Localized Sensor Positioning Systems

Bruce Barrow, SAIC

In September of 2006, a Geonics EM61-HH was used to interrogate a selection of the Calibration Grid buried inert ordnance at the Aberdeen Proving Ground Standardized Test Site. The EM61-HH sensor was swept back and forth over known object locations and positioning for this 3-D sensor trajectory was measured with an inertial measurement system being developed by ENSCO. On a subset of this data, the EM61-HH sensor was simultaneously tracked with the Arcsecond (now Metris) laser-based positioning system. Previous work with this laser-based tracking of the EM61-HH resulted in high quality model-based inversion of the sensor data and indicated that the positioning was accurate to a sub-centimeter level [1]. We will present here a comparison of the sensor trajectories measured by the two systems and the results of fitting the EM61-HH data using each trajectory. Typically, agreement between the two systems was found to be good to within 1-3 cm. The fit qualities with each positioning system were consistent with a < 1 cm positioning accuracy with the Arcsecond positioning giving noticeably better results.

Data Collection

The Aberdeen Calibration Grid is set up into rows A through K and columns 1 through 15 increasing from the NE corner of the grid. The smaller buried items are separated by 2 meters. For this test, a selection of items at shallower depths was interrogated, because of the limitations on the EM61-HH's detection of deep objects and the overly challenging depths used on the Calibration Grid. The items covered were 20mm, 40mm grenade, 57mm, 60mm mortar, 2.75 inch rocket warhead, 81mm mortar, 105mm, 155mm, and a shot-put. For the most part, three examples of each item were interrogated using only the ENSCO inertial system. Each interrogation over a given object was repeated at least three times; resulting in three independent data sets over each object. A 20mm at the grid location A3 was measured repeatedly with both the ENSCO and Arcsecond system. In this case, five measurements were taken in the morning and then five more in the afternoon.

The Arcsecond system used involved a set of four fixed transmitter stations and four receivers attached to the EM61-HH. After a calibration set up, the system collects data to track the EM61-HH coil head in 3-D along with orientation angles of yaw, pitch, and roll. The actual full trajectory at a 20 Hz data rate is only available in post-processing of the receiver measurements. The current post-processing only provides the trajectory in a local Arcsecond frame of reference based on the location of the fixed transmitters. In order to map the Arcsecond data to either the local APG grid or to UTM coordinates a surveyed point in the northeast corner of the site and a set of known grid points were measured with the Arcsecond system.

The ENSCO inertial system integrates measurements from a high quality inertial measurement unit (IMU). The integration starts and stops from a given "zero point". All data is relative to this zero point. The direction of the ENSCO local coordinates is determined by an electronic compass used by the system. In order to interrogate all of the cells across the site, four different zero points were used. To translate from ENSCO's local coordinates to Arcsecond's, these zero

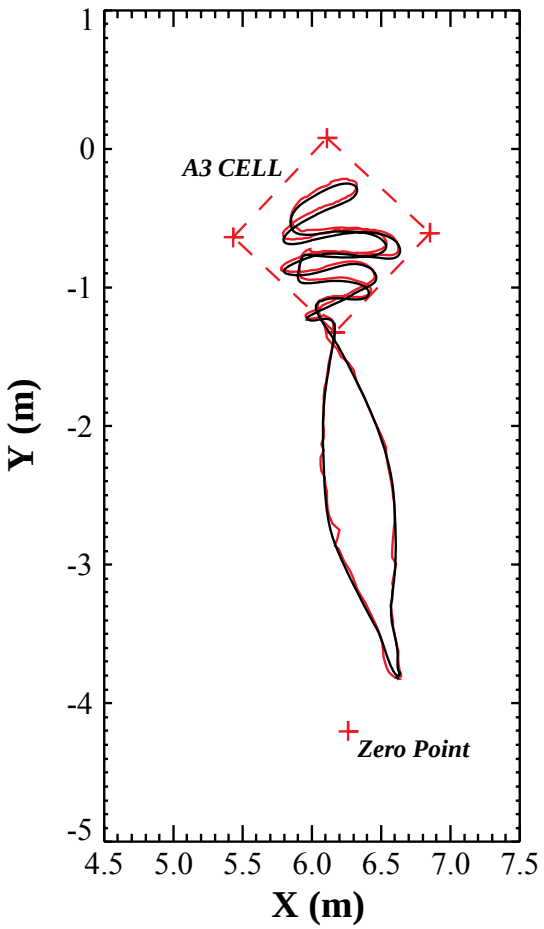

Figure 1. EM61-HH coil head trajectory over A3 cell in Arcsecond coordinate system. IMU trajectory is plotted in black and Arcsecond trajectory in red.

points were measured with the Arcsecond. The IMU raw data is collected at 600 Hz. After post-processing this data to an actual trajectory (*x, y, z, yaw, pitch, and roll*), ENSCO down sampled the position results to 20 Hz. The ENSCO data was provided in a positive z pointing down coordinate system and had to be converted to match the upward z pointing system used by the Arcsecond and the EM fitting algorithms.

The EM61-HH data was collected on the standard handheld computer provided by Geonics. The data was collected at a data rate of 15 Hz. The Geonics handheld has a second COM port to collect standardized GPS data. ENSCO is working on using this port to provide time stamping between the IMU data and the EM61-HH data. At the time of this data collection, this was not working properly. There was no attempt at all to synchronize the Arcsecond data to the Geonics data. In both cases, the EM61-HH data was manually shifted to within a second of the other systems. The EM fitting algorithm accounted for the residual time difference by adding it in as a fit parameter.

Trajectory Comparisons

To compare the two measured trajectories, the ENSCO data was shifted in time, shifted in space, and rotated to best match the Arcsecond trajectory. The time shift is due to the two different data acquisition clocks used by the systems. The spatial shift was based on the ENSCO zero point measured by the Arcsecond. For the ten common data sets, roughly the same rotation angle provided a good match between the two sets of data. The average angle was 41.2 degrees counter-clockwise to match the ENSCO data to the Arcsecond. The angles ranged from 40.1 to 42.05 with a standard deviation of 0.6. Figure 1 plots a comparison of the two trajectories in the *x, y* plane for one of the joint data collections over the A3 cell location. The black curve is from the ENSCO system and the red is from the Arcsecond. The red plus signs are measured grid and zero point locations.

To match the UTM coordinate system, a variety of local grid points was measured by the Arcsecond. Based on these, the Arcsecond coordinates must be rotated 35.9 degrees clockwise to align with true north. From this, the ENSCO coordinates needed to be rotated 5.3 degrees counter-clockwise to match UTM.

Using the average rotation angle and zero point, Figure 2 plots the ENSCO only trajectories from the same zero point. This time the data is in the local grid coordinates relative to the northeast corner of the A1 cell. The red curve is from a common Arcsecond/ENSCO trajectory. The black curves are all from ENSCO only data collections. The red plus signs are fixed grid points measured by the Arcsecond system. For these ENSCO only trajectories, there appears to be some further rotation and possibly shift required to get them to match the actual measured cell location. Figure 3 plots similar results from two other zero points.

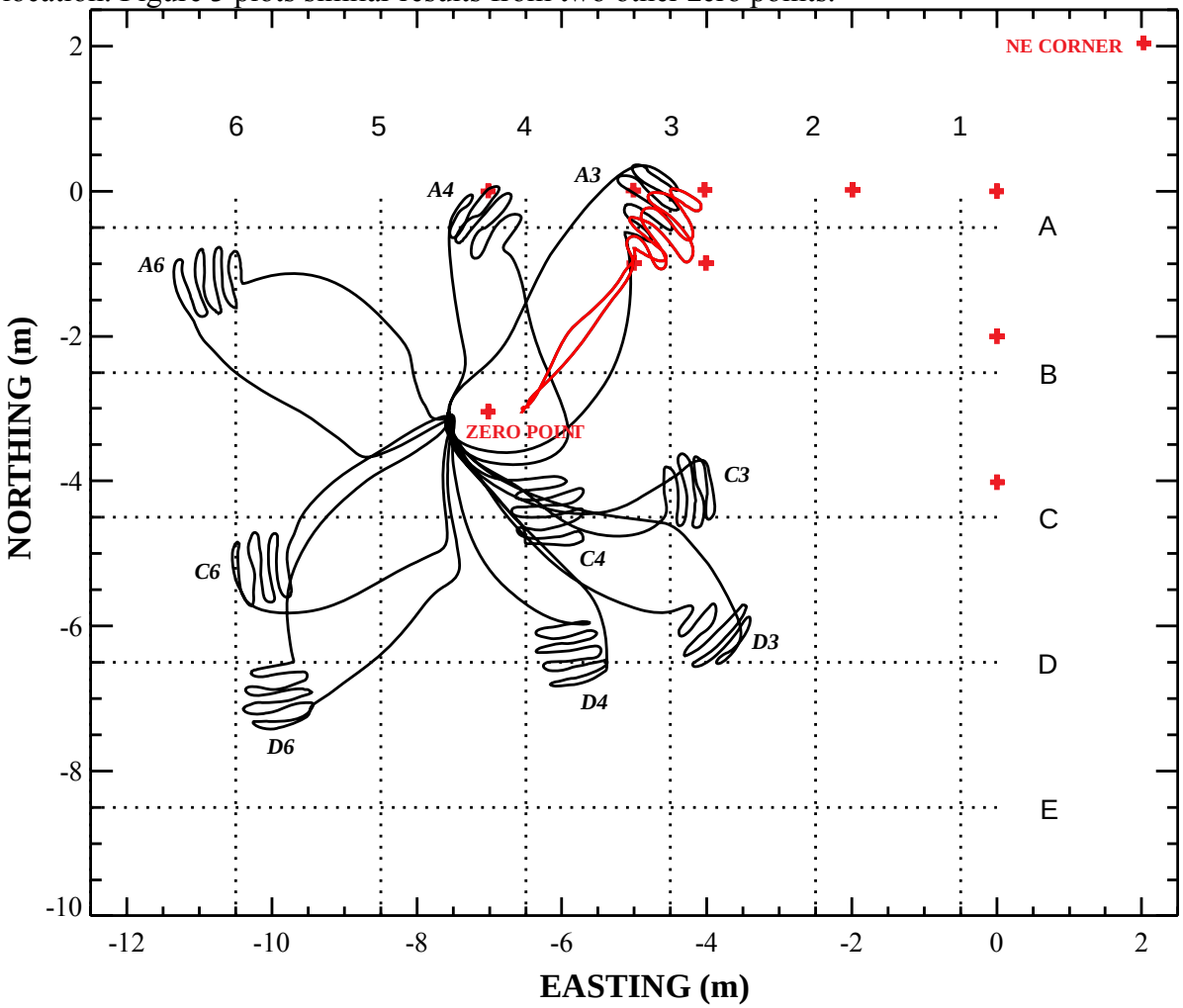

Figure 2. Different cell trajectories about zero point and relative to APG local grid. Joint Arcsecond/IMU data in red and IMU only data in black.

Figures 4 and 5 graph comparisons of joint Arcsecond/ENSCO trajectories in more detail. In 4(a) and 5(a), the Arcsecond trajectory is plotted in red and ENSCO is in black. The other graphs plot (b) the horizontal and (c) vertical distances between the two trajectories as a function of time. In Figure 4 there is very close agreement and in Figure 5 there is not. The Arcsecond system typically jitters about the true trajectory, and occasionally spikes way off when one or more receivers are blocked. However, its absolute positioning over time tends to be very good. The ENSCO data plots a very smooth trajectory, but appears to drift off from the ARCSECOND trajectory. Out of the ten joint trials, eight of them drifted off on the order of one to three

centimeters in the horizontal similar to the example in Figure 4. For two of the trials, the ENSCO trajectory drifted way off, and the extent of the drift varied over time as in Figure 5. Comparing the orientation angles between the two showed similar results with typical differences in orientation being on the order of only several degrees or less. Statistics for the differences in position and orientation of the two trajectories are presented in Table I for all ten runs.

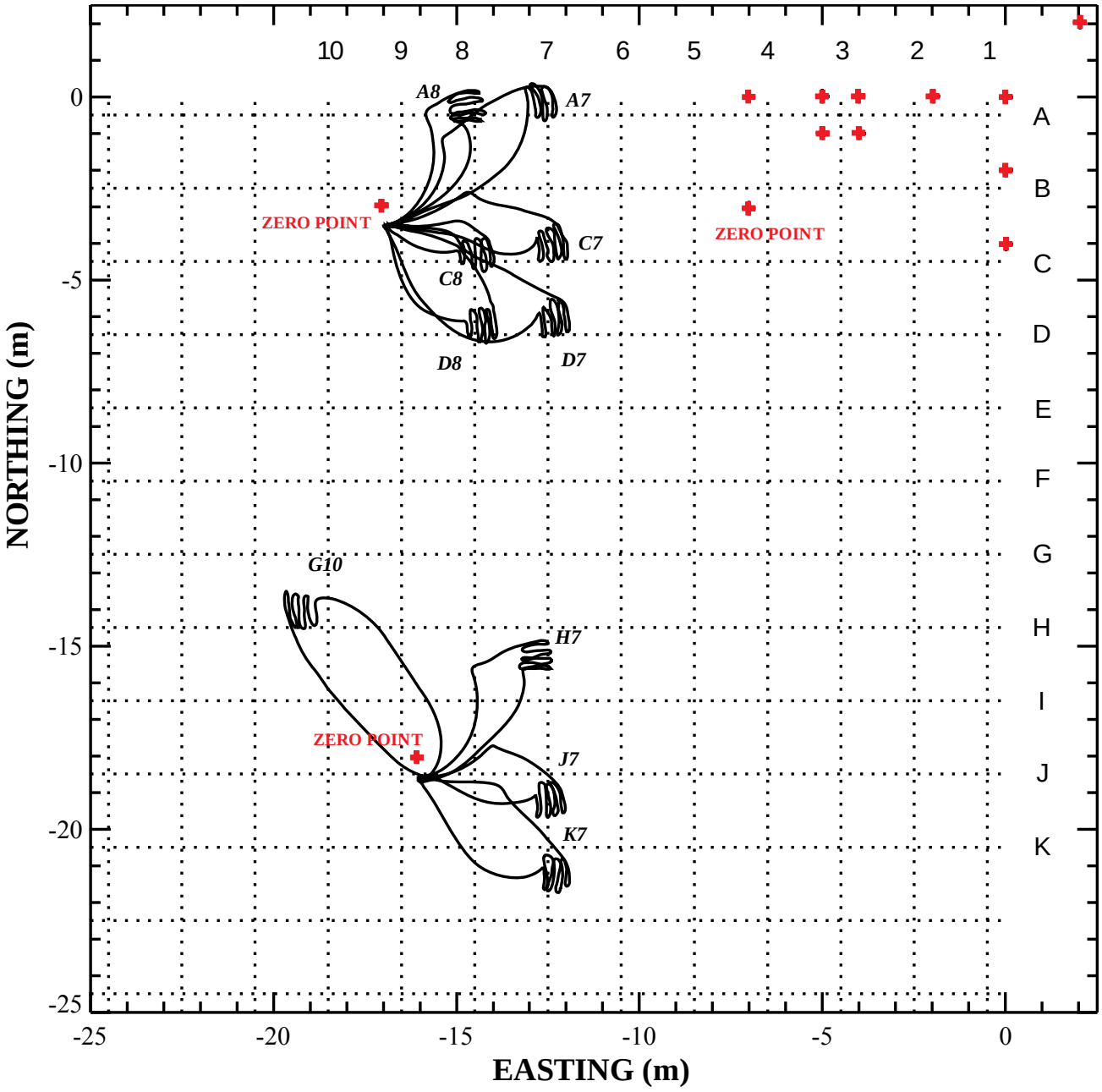

Figure 3. Different cell trajectories from IMU only data at other Arcsecond measured zero points. Local grid coordinates.

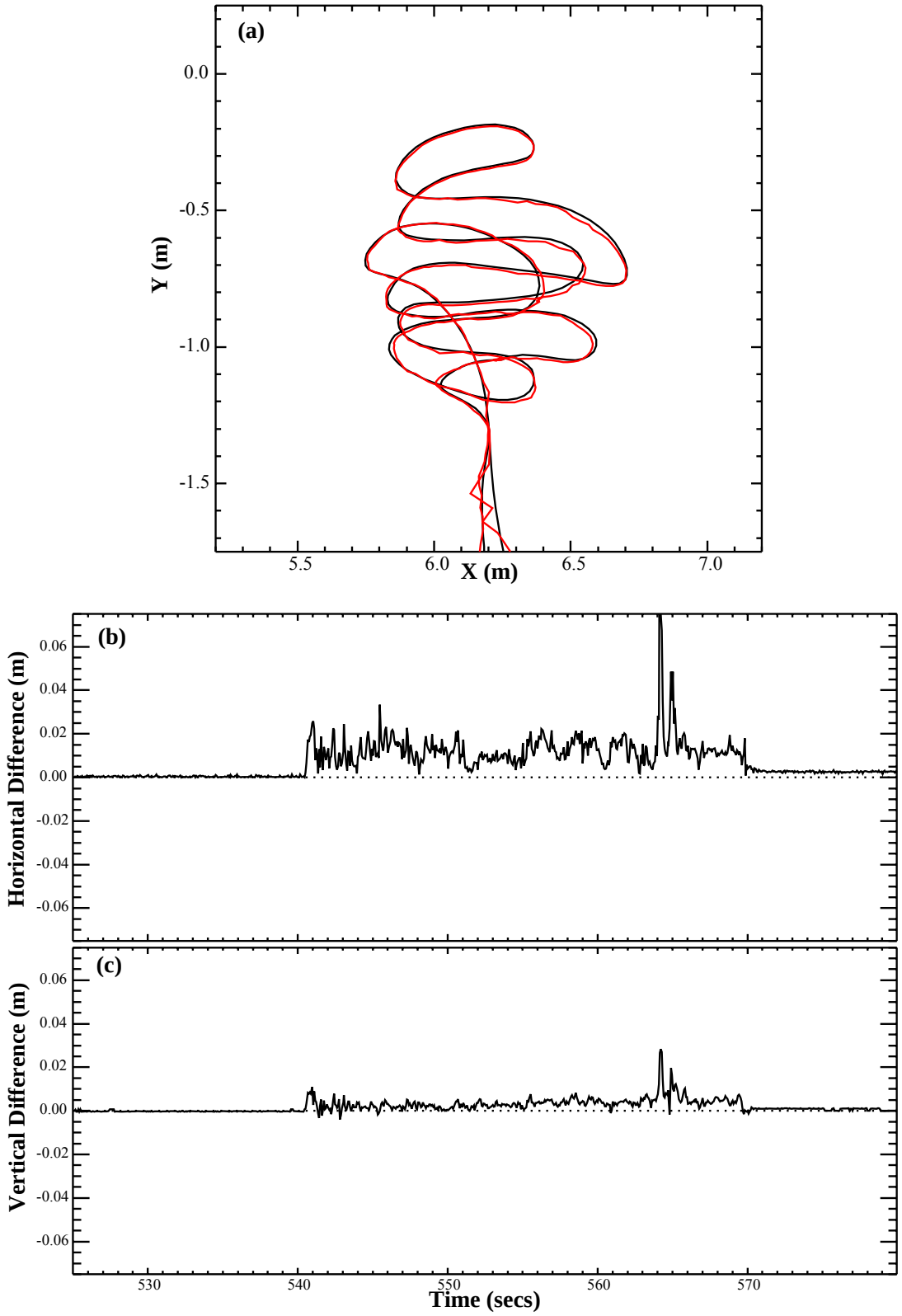

Figure 4. Comparison of IMU (black) and Arcsecond (red) trajectories. Arcsecond coordinates.

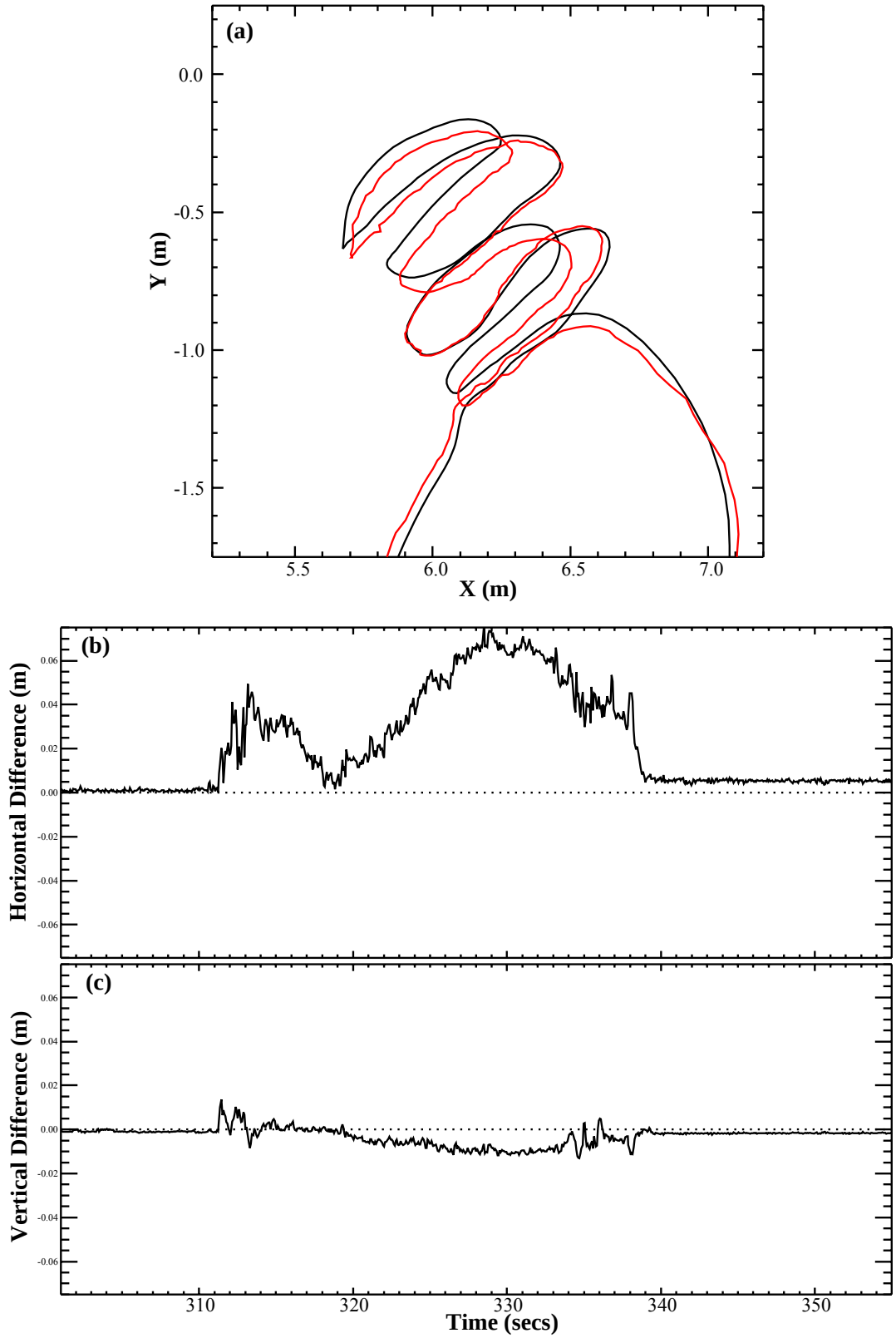

Figure 5. Second comparison of IMU (black) and Arcsecond (red) trajectories. Arcsecond coordinates.

Table I. Differences between Arcsecond and IMU Trajectories.

		Difference in X (m)	Difference in Y (m)	Horizontal Difference (m)	Difference in Z (m)	Difference in Yaw (degs)	Difference in Pitch (degs)	Difference in Roll (degs)
Run #1	Mean	-0.002	0.001	0.017	-0.005	1.96	-2.41	-1.37
	Standard Deviation	0.018	0.013	0.014	0.006	0.86	0.61	0.47
Run #2	Mean	-0.001	-0.006	0.013	-0.003	1.83	-2.45	-1.33
	Standard Deviation	0.011	0.008	0.009	0.003	0.74	0.40	0.35
Run #3	Mean	-0.004	0.044	0.046	-0.004	1.62	-2.56	-1.33
	Standard Deviation	0.007	0.020	0.017	0.002	0.62	0.31	0.27
Run #4	Mean	-0.002	0.022	0.027	-0.003	1.58	-2.46	-1.31
	Standard Deviation	0.012	0.011	0.007	0.003	0.60	0.32	0.31
Run #5	Mean	-0.003	0.025	0.028	-0.002	1.65	-2.49	-1.37
	Standard Deviation	0.007	0.013	0.009	0.002	0.73	0.27	0.28
Run #6	Mean	-0.003	0.017	0.020	-0.003	0.79	-1.13	-0.62
	Standard Deviation	0.007	0.009	0.008	0.003	0.64	0.27	0.39
Run #7	Mean	0.000	0.000	0.008	-0.005	0.85	-1.04	-0.66
	Standard Deviation	0.007	0.007	0.005	0.002	0.41	0.19	0.21
Run #8	Mean	-0.006	0.026	0.028	-0.002	0.73	-1.21	-0.71
	Standard Deviation	0.007	0.011	0.010	0.005	0.69	0.56	0.39
Run #9	Mean	0.000	-0.001	0.012	-0.004	0.94	-1.09	-0.62
	Standard Deviation	0.013	0.010	0.012	0.003	0.85	0.38	0.52
Run #10	Mean	0.011	-0.024	0.039	0.005	1.45	-1.14	-0.66
	Standard Deviation	0.027	0.022	0.021	0.005	0.67	0.25	0.29
OVERALL	Average Mean	-0.001	0.010	0.024	-0.003	1.341	-1.798	-0.997
	Average Standard Deviation	0.012	0.012	0.011	0.003	0.680	0.356	0.347

Model-Based Inversion

The basic electromagnetic induction response model involves a simple dipole response [2]. Inversion of this model solves for the object's location, object orientation, and the magnetic polarization response terms. The polarization terms, referred to here as β's, determine the strength of the object's induced response along the object's physical axes. It is these terms that allow for discrimination between buried ordnance and other metallic clutter. For elongated ferrous ordnance items such as a projectile or mortar, there is one large, primary β response along the item's long axis and two smaller, secondary responses transverse to this, $\beta_x > \beta_y = \beta_z$. Accurately determining these parameters from model-based inversion is limited by the signal-to-noise ratio (SNR) of the sensor data and by the positioning accuracy of the sensor trajectory. In simulations [1], positioning accuracy of better than 1 centimeter is required to invert β's with less than 20% error.

There are several other complications in inverting the EM61-HH data combined with the IMU trajectory. The first is the added requirement for modeling the sensor's dynamic time response. The receiver output of this sensor is analog integrated with a filter that both shifts and distorts the sensor's response. This filter has been added to the forward model used by the inversion algorithm. It is possible that this filter is sufficiently distorting signal shape to limit the inversion

process. The second complication is the sensor bias drift. Over minutes of data collection, the zero level of the sensor will change. The data collected here starts with the sensor on a metal tripod with an unknown offset. It then moves back and forth over an object perhaps reaching zero at points, perhaps not. Because of this, an offset parameter has been added to the data inversion. Lastly, the EM data is not synchronized with the IMU data. A time difference term is yet another fit parameter.

Besides the fit parameters, the inversion algorithm returns a reduced chi-squared value for the fit and a squared correlation coefficient, R^2, between the best model fit and the measured data. The dipole fit error is expressed as $\sqrt{1-R^2}$. The percentage fit error grows with both low SNR signals and with poor positioning. For the ten separate measurements made over the A3 cell, the EM61-HH data was inverted first using the Arcsecond positioning and then using the IMU positioning. Figure 6 plots the fit error results for one positioning system versus the other using the same EM data. For half of the data, the two systems result in comparable fit errors. For the two data sets where the trajectories did not match well, the IMU fit errors are significantly greater.

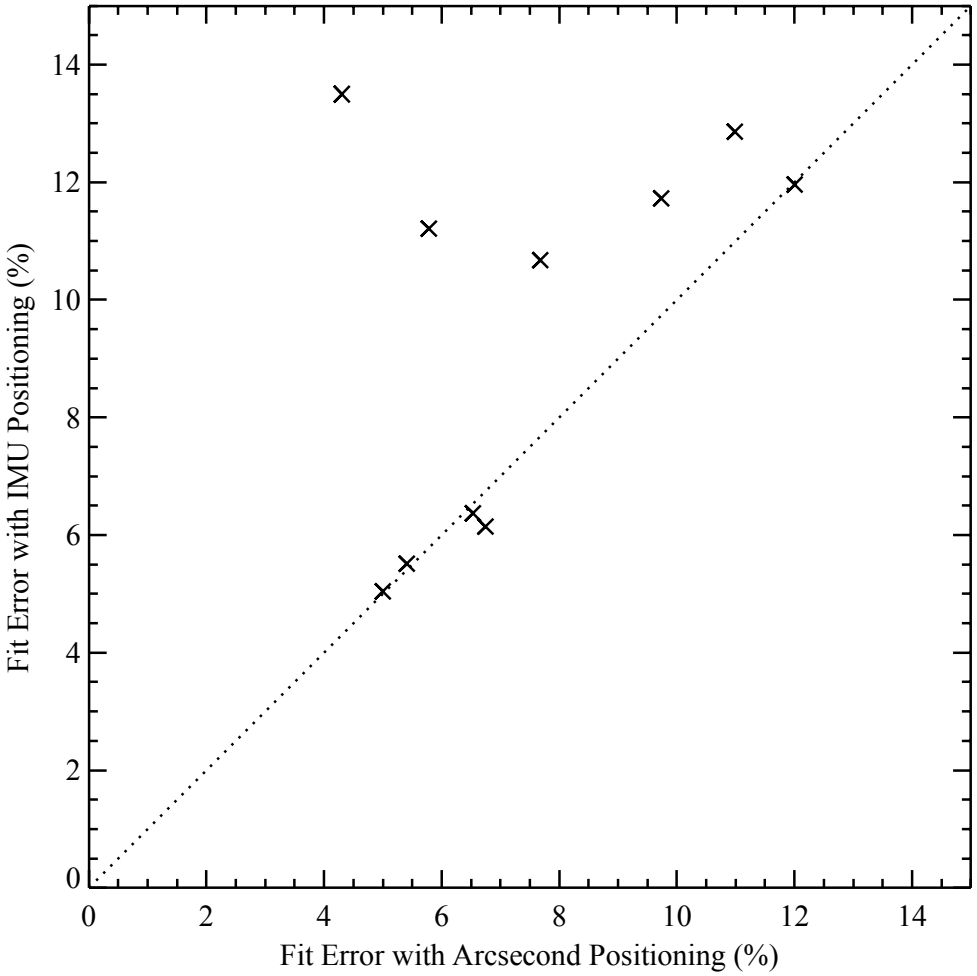

Figure 6. Fit error comparison between EM data with IMU and Arcsecond positioning.

Figure 7 plots the spread in the inverted β parameters over all 20mm measurements. In these plots, the *x* axis plots the largest β value from the fit. The *y* axis plots the average (diamond symbol) and the range (vertical line) of the two secondary β values. For axisymmetric objects like the 20mm, the secondary β's should be equal and the vertical line should be a dot. The points in 7(a) are from fits using Arcsecond positioning. The mean primary β value is 0.387 with a standard deviation of 0.028 (7% of mean). The average secondary value is 0.110 with a standard deviation of 0.014 (13%). The same fits with IMU positioning are shown in 7(b). The mean value is 0.370 with a standard deviation of 0.059 (16%). The secondary mean is 0.105 with a standard deviation of 0.024 (23%). The spread in the β fits is roughly twice as great for the IMU positioning. Similar increased spreads in the other object fit parameters (*x, y* location and depth) were observed with the IMU positioning.

Figure 7(c) plots the fit results for IMU only measurements made over the 20mm cells: A3, C3, and D3. The results are comparable to 7(b). Figure 8 plots the fit results for data collected over the A4, C4, and D4 cells containing a 40mm grenade. These results are plotted in black with diamond symbols. For comparison, the 20mm results are plotted in red. There are comparable spreads in this data, but it is sufficiently small to discriminate between the two items. It should be noted that one fit result is significantly off and that another data set failed to fit successfully.

Figure 9 plots the fit error versus the SNR of the EM61-HH signal from these data sets: joint 20mm Arcsecond (green X) / IMU (red X), 20mm IMU only (black diamond), and 40mm grenade IMU only (blue triangle). The general trend is for decreasing fit error with increasing SNR. The solid black curve is a calculated limit for fit error as a function of SNR assuming no position errors [3]. The dotted curves plot the limits assuming position errors on the order of one and two centimeters. The bulk of the fits fall under the one centimeter curve.

The rest of the data collected over other cells on the APG calibration grid had signals in the range of 0 to 30 dB. With an RMS noise level of 4 millivolts, this is in the range of 0 to 200 millivolts. The inversion algorithm had trouble converging to a solution for data in the 20 to 30 dB range. In some cases, several local minima were found by the fit algorithm.

Conclusions

The majority of the joint Arcsecond and ENSCO IMU positioning data showed agreement in the horizontal sensor head trajectories to be within one to three centimeters (see Table I). There were two data sets where the ENSCO IMU data was found to drift significantly off from the Arcsecond horizontal positioning. The EM fits resulting from these two systems showed general agreement, with the Arcsecond showing a smaller spread in the fit parameters (7% to 13% variations about the mean response β's versus 16% to 23%). Even with the larger spread in β's, the IMU positioned fits are sufficient to discriminate between a 20mm projectile and a 40 mm grenade. Comparisons of the fit results overall are promising with the bulk of the fit errors falling about theoretical curves indicating roughly one centimeter relative positioning error (figure 9).

Possible testing and improvements do remain to be made. There is no current explanation for the two data runs that drifted significantly off. There was nothing indicated in the IMU output to flag

them as being poor. The EM fits were of poorer, but not unreasonable, quality (10-14% versus 5-10%). The fit algorithm did have trouble converging for this data and there were several β parameter outliers. Further data collections on a large set of objects (ordnance and clutter) with both high and low SNR signals would be worth while. Study of such a data set may indicate how to flag bad positioning and bad EM fit runs and how to best use the fit parameters for discrimination.

References

[1] B. Barrow, T. Bell, and N. Khadr, "Evaluation of Laser Based Positioning for Characterization of EMI Signals from UXO." Proceedings of SAGEEP Conference, Seattle, Wash., April 2006.

[2] T. Bell, B. Barrow, and J. Miller, "Subsurface Discrimination Using Electromagnetic Induction Sensors", IEEE Transactions on Geoscience and Remote Sensing, Vol. 39, no. 6, pgs 1286-1293, June, 2001.

[3] J. Kingdon, T. Bell, "Processing and Analysis Results for MM-1310 Blossom Point Demonstration", Technical Report provided to Shaw Environmental in support of SERDP Project MM-1310.

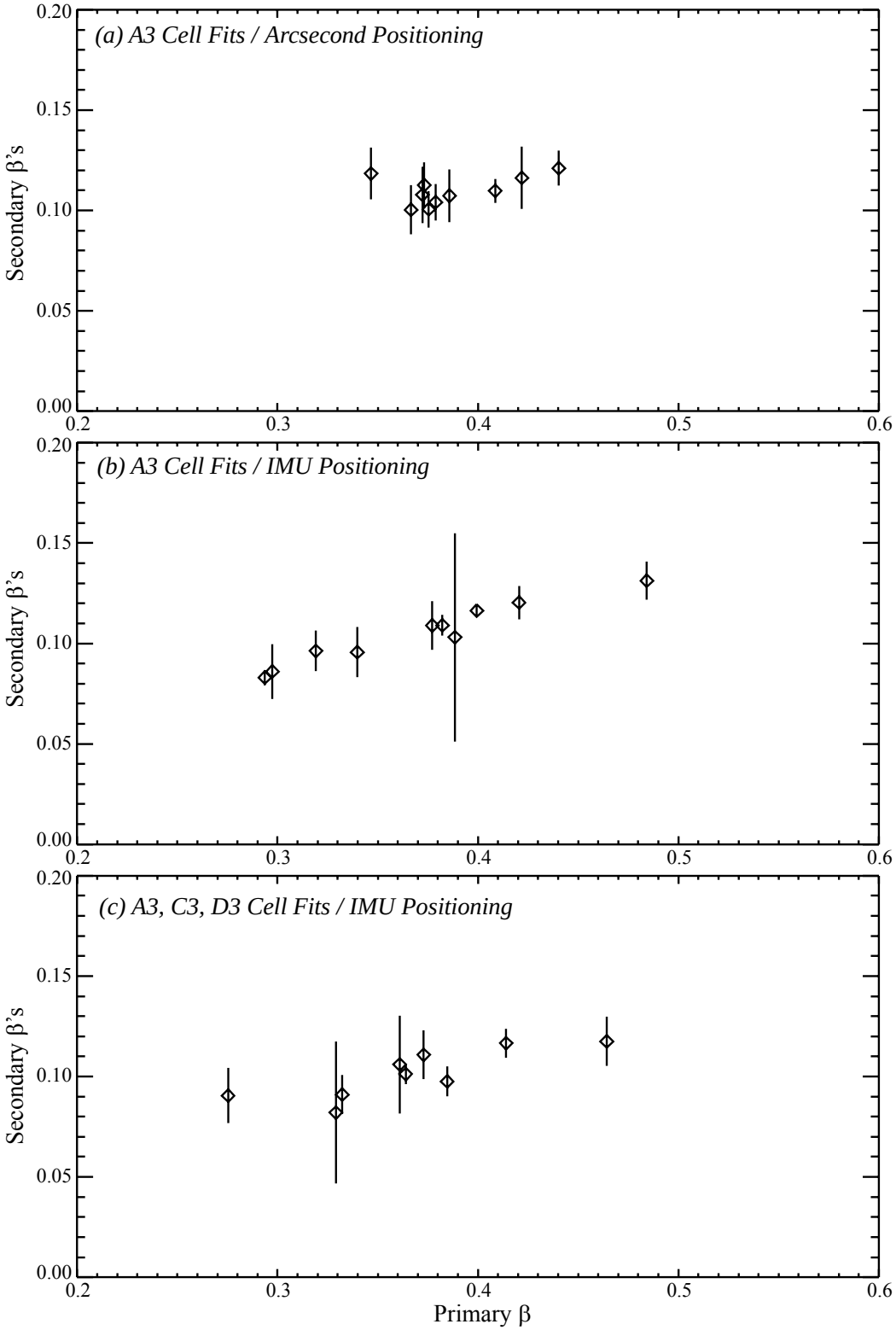

Figure 7. Comparison of fitted β polarization parameters on 20mm cells.

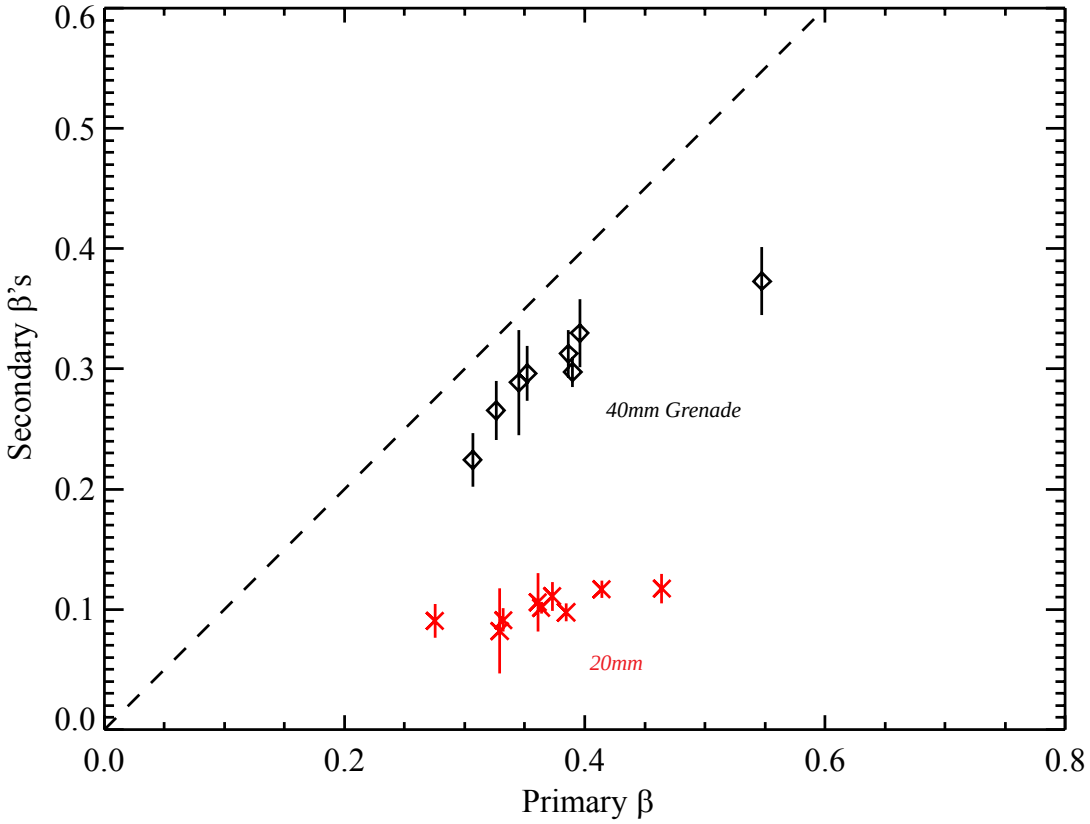

Figure 8. β fits of 40mm grenade data compared to 20mm fits.

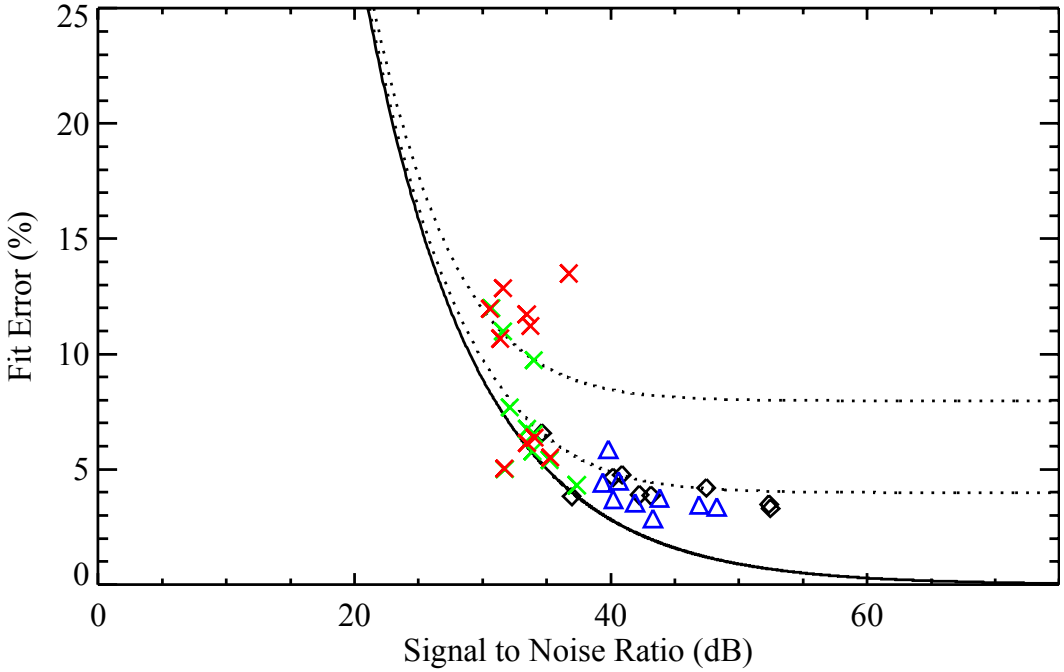

Figure 9. Plots of fit error versus EM61-HH signal-to-noise ratio. Curves indicate limits based on 0, 1, and 2 centimeter positioning errors.